Glucose and glycerol transport in adipocytes from a structural perspective

Huang, Peng

2022

Document Version:
Publisher's PDF, also known as Version of record

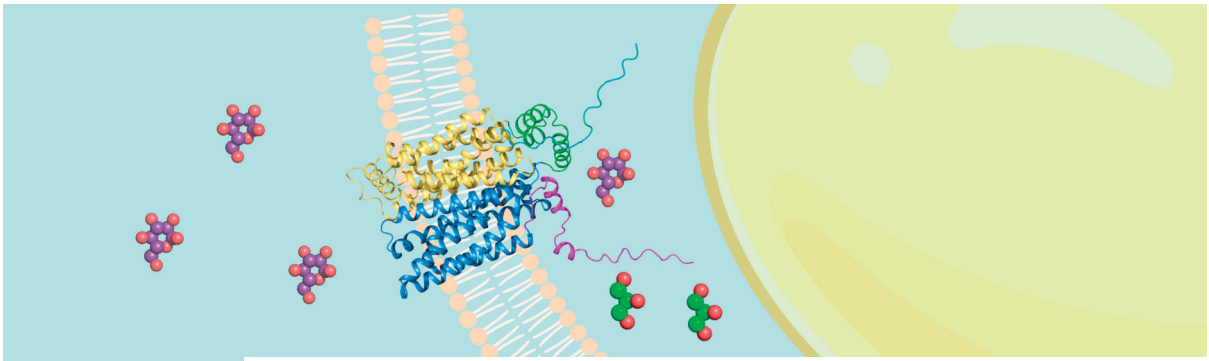

Glucose and glycerol transport in adipocytes from a structural perspective

PENG HUANG
EXPERIMENTAL MEDICAL SCIENCE | FACULTY OF MEDICINE | LUND UNIVERSITY

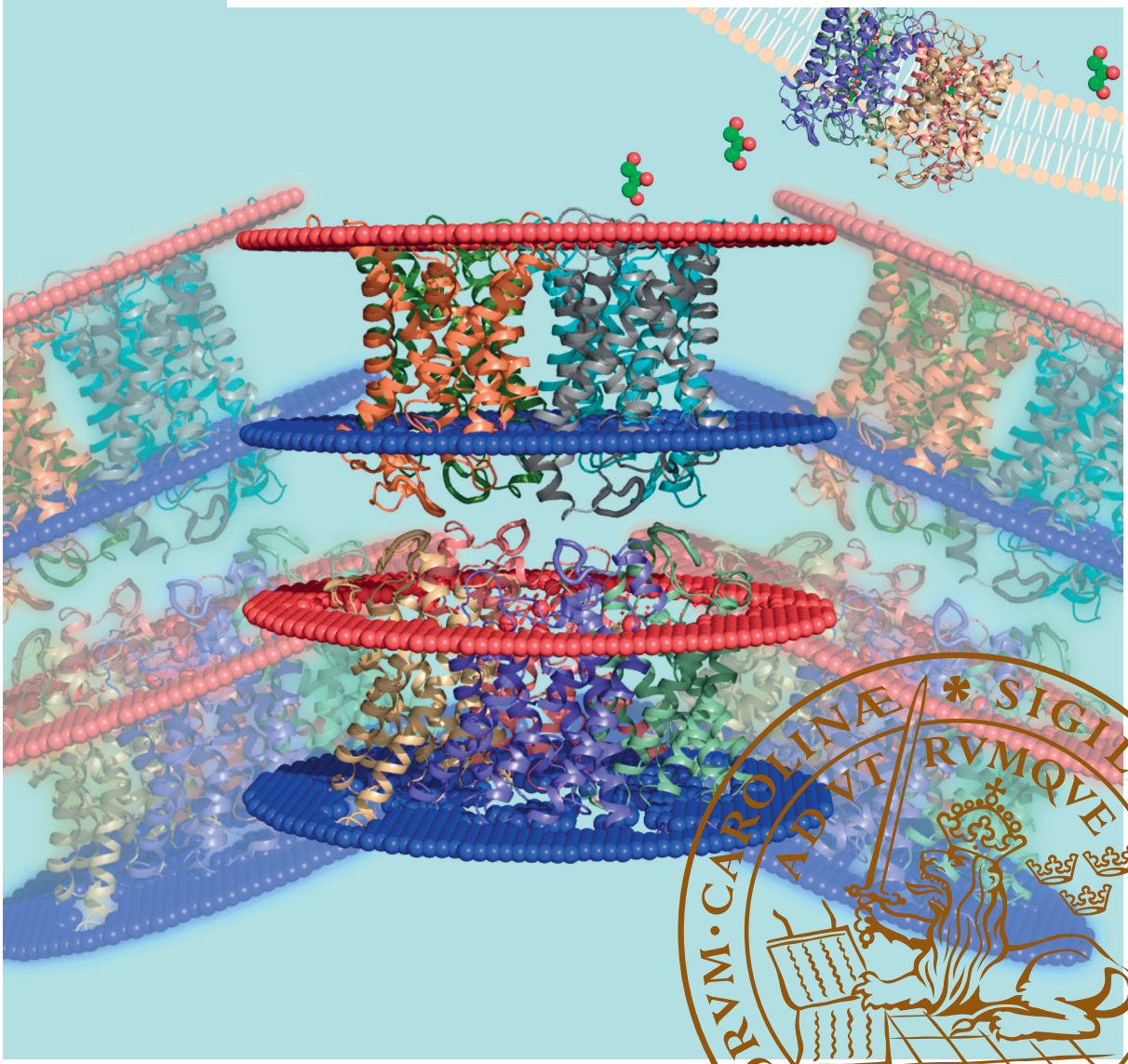

Printed by Media-Tryck, Lund 2022 NORDIC SWAN ECOLABEL 3041 0903

LUND UNIVERSITY

FACULTY OF MEDICINE

Department of Experimental Medical Science

Lund University, Faculty of Medicine
Doctoral Dissertation Series 2022:8
ISBN 978-91-8021-169-7
ISSN 1652-8220

Glucose and glycerol transport in adipocytes from a structural perspective

Glucose and glycerol transport in adipocytes from a structural perspective

Peng Huang

LUND
UNIVERSITY

DOCTORAL DISSERTATION

by due permission of the Faculty of Medicine, Lund University, Sweden.
To be defended on January 27, 2022, at 13:00 in Segerfalksalen, BMC, Lund

Faculty opponent
Prof. David Drew

Stockholm University

Organization LUND UNIVERSITY	Document name Doctoral dissertation
	Date of issue January 27 2022
Author(s): Peng Huang	Sponsoring organization

Title and subtitle Glucose and glycerol transport in adipocytes from a structural perspective

Abstract

Adipocytes are crucial energy reservoirs to maintain metabolic homeostasis of glucose and lipids in the human body. Glucose transporters (GLUTs) and aquaporins (AQPs) play an important role in metabolic regulation of glucose and lipids in human adipocytes. Specifically, glucose transporter 4 (GLUT4) and aquaporin 7 (AQP7) are the central players for glucose transport and glycerol efflux in adipocytes. In addition, GLUT family members are overexpressed in a vast majority of cancer cells to satisfy their increased energy demand, thus, inhibitors targeting GLUTs are becoming relevant therapeutics for cancers treatment. To control the uptake/release of nutrients, GLUTs and AQPs have been suggested to be controlled by trafficking mechanisms. TUG (tether containing UBX domain for GLUT4 in mouse) and PLIN1 (human perilipin 1) have previously been suggested to bind with GLUT4 and AQP7 intracellularly and release them upon hormonal stimulation. Here, the mRNA expression levels of GLUTs and AQPs in adipose tissue has been investigated, and detailed characterization of the interaction between GLUT4 and ASPL (human TUG homolog) and AQP7 and PLIN1 in vitro have been executed. In addition, a new series of glucose transporter 1 (GLUT1) inhibitors was structurally and functionally investigated. Finally, the AQP7 structure was elucidated by single particle cryo-EM.

In this thesis I suggest that GLUT4 interacts with ASPL using its intracellular helical domain to bind to the C-terminus of ASPL. Rat GLUT4 was expressed in Pichia pastoris, and purified, and showing even single-particle distribution in negative staining, providing insight on further structural study of GLUT4 by single particle cryo-EM. Docking models of the complex of GLUT4 and ASPL were generated and suggest that ASPL forms complex with GLUT4 by multiple domains including both ubiquitin-like domain (UBL2) and ubiquitin domain (UBX). In addition, PGL13 and PGL14, as new series of GLUT1 inhibitors were suggested to utilize two sites of GLUT1, the transmembrane domain and intracellular helical domain. Moreover, in human adipocytes AQP7 gene showed markedly higher-level expression than other aquaglyceroporins. The C-terminal domain of PLIN1 was suggested to be central for the complex formation with AQP7 and AQP3. The AQP7 structure was determined at the resolution of 2.55 Å by cryo-EM, adopting the formation of dimer of tetramers. Two tetramers were dimerized by extracellular protruding C loops with a rotation of approximate 11° around central axis. The central pore is formed by four monomers and restricted by two leucine filters. Moreover, well-defined densities were discovered in the central pores showing decent fitting with some small metabolic products.

Key words adipocytes, glucose and glycerol metabolism, glucose transporters, aquaglyceroporins, glucose transporter 4, aquaglyceroporin 7, protein and protein interaction, structure, single particle cryo-EM

Classification system and/or index terms (if any)

Supplementary bibliographical information		**Language** English
ISSN 1652-8220 Faculty of Medicine Doctoral Dissertation Series 2022:8		**ISBN** 978-91-8021-169-7
Recipient's notes	**Number of pages** 85	Price
	Security classification	

Signature Peng Huang Date 2021-12-13

Glucose and glycerol transport in adipocytes from a structural perspective

Peng Huang

LUND
UNIVERSITY

Coverphoto by Peng Huang

Faculty of Medicine
Department of Experimental Medical Science

ISBN 978-91-8021-169-7
ISSN 1652-8220

Printed in Sweden by Media-Tryck, Lund University
Lund 2022

Dedicated to my beloved wife and child

If there is a will, there is a way

有志者，事竟成

Table of Contents

Popular summary

Sugar from food is necessary for cell growth in the human body, however, when too much sugar is ingested, it will be converted to fat and stored in the fat cells. After exercising or fasting, the fat is broken down into fatty acids and glycerol, which is called lipolysis. The sugar uptake into fat cells is controlled by sugar transporters, while upon lipolysis glycerol is exported by glycerol channels (Fig. 1). If sugar transporters do not take up the sugar, it will stay in the blood stream and lead to diabetic symptoms. On the other hand, if the glycerol channels lose their functions, the fat is accumulated in fat cells and may lead to obesity. The sugar transporters and the glycerol channels are membrane proteins, which can be visualized as gates to control uptake and release of nutrients. All cells in human body are parcelled by cell membrane like a shell (Fig. 1). The membrane not only protects cells from the outside environment, but also accommodates a lot of proteins performing many functions important for cell growth and surviving. These proteins are called membrane proteins, and they function, sometimes, by coupling to other proteins, a behaviour called proteins interactions. We aim to study how sugar transporters and glycerol channels look like by microscopic technique, to learns more about their function, and how they are coupled with their interaction partners, to facilitate deeper understanding of diseases like diabetes and obesity.

Moreover, cancer cells acquire more sugar transporters to take up sugar from the blood to grow. Here, we have analysed inhibitors which can inhibit sugar to enter cells by blocking the transporters (Fig.1). As a result, cancer cells became more sensitive to standard chemotherapy, and thus these inhibitors are promising candidate to be applied in the clinic to prevent cancer development.

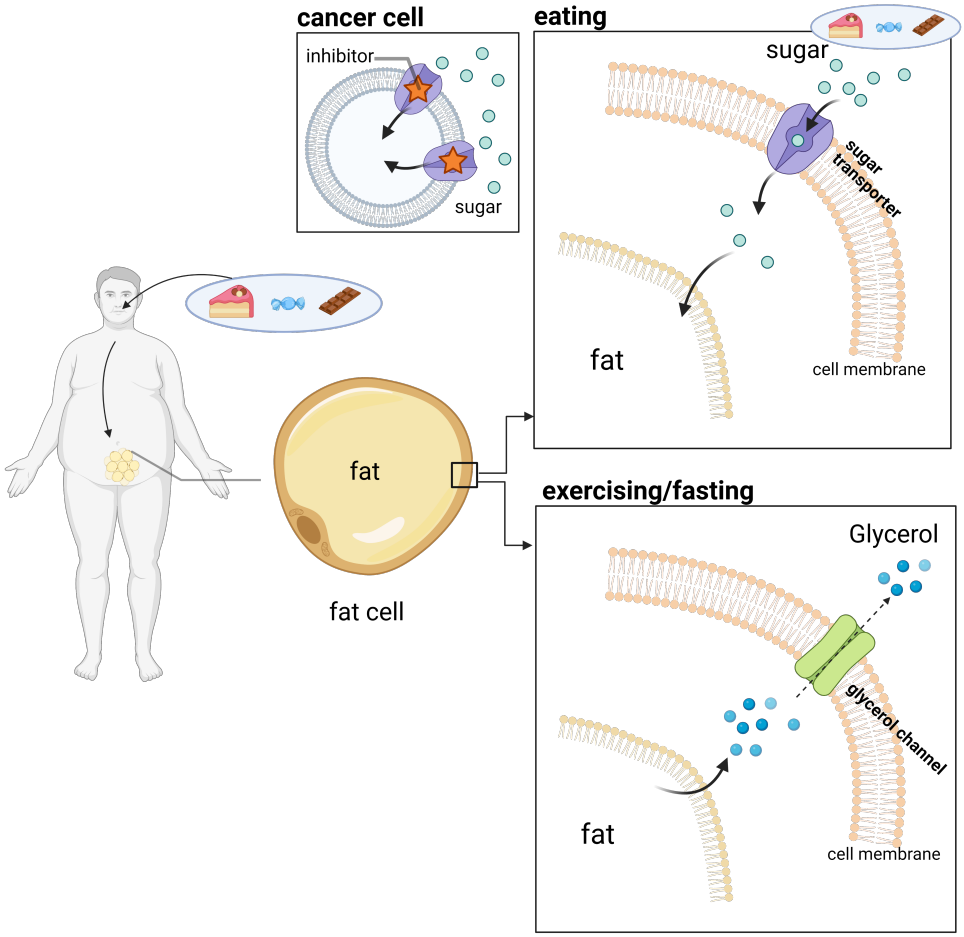

Figure 1. Schematic representation of the transport of sugar and glycerol in fat cells and the inhibition of sugar supply in cancer cells. Created with BioRender.com.

Abstract

Adipocytes are crucial energy reservoirs to maintain metabolic homeostasis of glucose and lipids in the human body. Glucose transporters (GLUTs) and aquaporins (AQPs) play an important role in metabolic regulation of glucose and lipids in human adipocytes. Specifically, glucose transporter 4 (GLUT4) and aquaporin 7 (AQP7) are the central players for glucose transport and glycerol efflux in adipocytes. In addition, GLUT family members are overexpressed in a vast majority of cancer cells to satisfy their increased energy demand, thus, inhibitors targeting GLUTs are becoming relevant therapeutics for cancers treatment. To control the uptake/release of nutrients, GLUTs and AQPs have been suggested to be controlled by trafficking mechanisms. TUG (tether containing UBX domain for GLUT4 in mouse) and PLIN1 (human perilipin 1) have previously been suggested to bind with GLUT4 and AQP7 intracellularly and release them upon hormonal stimulation. Here, the mRNA expression levels of GLUTs and AQPs in adipose tissue has been investigated, and detailed characterization of the interaction between GLUT4 and ASPL (human TUG homolog) and AQP7 and PLIN1 *in vitro* have been executed. In addition, a new series of glucose transporter 1 (GLUT1) inhibitors was structurally and functionally investigated. Finally, the AQP7 structure was elucidated by single particle cryo-EM.

In this thesis I suggest that GLUT4 interacts with ASPL using its intracellular helical domain to bind to the C-terminus of ASPL. Rat GLUT4 was expressed in *Pichia pastoris*, and purified, and showing even single-particle distribution in negative staining, providing insight on further structural study of GLUT4 by single particle cryo-EM. Docking models of the complex of GLUT4 and ASPL were generated and suggest that ASPL forms complex with GLUT4 by multiple domains including both ubiquitin-like domain (UBL2) and ubiquitin domain (UBX). In addition, PGL13 and PGL14, as new series of GLUT1 inhibitors were suggested to utilize two sites of GLUT1, the transmembrane domain and intracellular helical domain. Moreover, in human adipocytes AQP7 gene showed markedly higher-level expression than other aquaglyceroporins. The C-terminal domain of PLIN1 was suggested to be central for the complex formation with AQP7 and AQP3. The AQP7 structure was determined at the resolution of 2.55 Å by cryo-EM, adopting the formation of dimer of tetramers. Two tetramers were dimerized by extracellular protruding C loops with a rotation of approximate 11° around central axis. The central pore is formed by four monomers and restricted by two leucine filters.

Moreover, well-defined densities were discovered in the central pores showing decent fitting with some small metabolic products.

List of publications

Paper I

Peng Huang, Hannah Åbacka, Daniel Varela, Raminta Venskutonyte, Lotta Happonen, Pontus Gourdon, Mahmod R Amiry-Moghaddam, Ingmar André, Karin Lindkvist-Petersson. **ASPL is expressed in human adipocytes and can form complex with the intracellular helical bundle of human GLUT4**. Manuscript.

Paper II

Peng Huang, J.S. Hansen, K.H. Saba, A. Bergman, F. Negoita, P. Gourdon, A. Hagström-Andersson, K. Lindkvist-Petersson, **Aquaglyceroporins and orthodox aquaporins in human adipocytes**, Biochimica et Biophysica Acta (BBA) - Biomembranes 1864(1) (2022). 183795.

Paper III

H. Åbacka, J.S. Hansen, **P. Huang**, R. Venskutonytė, A. Hyrenius-Wittsten, G. Poli, T. Tuccinardi, C. Granchi, F. Minutolo, A.K. Hagström-Andersson, K. Lindkvist-Petersson, **Targeting GLUT1 in acute myeloid leukemia to overcome cytarabine resistance**, Haematologica 106(4) (2021) 1163-1166.

Paper IV

Peng Huang, Raminta Venskutonyte, Sofia de Maré, Xiao Fan, Ping Li, Pontus Gourdon, Nieng Yan, Karin Lindkvist-Petersson. **Single particle cryo-EM structure of human AQP7 adopts an octameric formation and shows novel features of the central pore**. Manuscript

Abbreviations

WAT	White adipose tissue
TAG	Triacylglycerol
BAT	Brown adipose tissue
TEM	Transmission electron microscopy
GLUTs	Glucose transporters
Gro3P	Glycerol-3-phosphate
AQPs	Aquaporins
DHAP	Dihydroxyacetone-3-phosphate
G3P	Glyceraldehyde-3-phosphate
MFS	Major facilitator superfamily
CoA	Coenzyme A
FAs	Fatty acids
VLDLs	Very low-density lipoproteins
CM	Chylomicrons
LPL	Lipoprotein lipase
ATGL	Adipocytes triglyceride lipase
HSL	Hormone sensitive lipase
MGL	Monoacylglycerol lipase
GK	Glycerol kinase
PKA/C	Protein kinase A/C
PPI	Protein and protein interaction
PLIN1	Perilipin 1
UBX	Ubiquitin domain
ICH	Intracellular helical bundle

Trx	Thioredoxin
ABDH5	AB-hydrolase-containing 5
SPR	Surface plasma resonance
XL-MS	Cross-linking mass spectrometry
BN-PAGE	Blue native PAGE
SEC	Size exclusion chromatography
PGLs	Salicylketoxime derivatives
Cryo-EM	Cryogenic electron microscopy
3D	Three dimension
IPP	Isopentenyl pyrophosphate
DMAPP	Dimethylallyl pyrophosphate
AML	Acute myeloid leukemia
PTM	Post-transcriptional modification
GDN	Glyco-diosgenin
CTF	Contrast transfer function
CMC	Critical micelle concentration
MSP	Membrane scaffold protein
DM	Decyl-β-D-maltopyranoside
DDM	Dodecyl-β-D-maltopyranoside
MNGs	Maltose-neopentyl glycols

Energy metabolism and regulation in human adipocytes

Adipose tissue plays important roles in maintaining carbohydrate and lipid homeostasis in the human body. The major fat depots in human consist of varying amounts of two different types of adipose tissue: white adipose tissue (WAT) that stores energy in the form of triacylglycerol (TAG), brown adipose tissue (BAT) that "burns" fatty acids to maintain body temperature. BAT is traditionally thought to be restricted to subcutaneous region of interscapular in new-borns and early childhood period, while in adults, BAT is primarily located in the cervical, axillary, and supraclavicular regions[8]. WAT is localized mainly in the abdominal and gluteal-femoral subcutaneous region as well as visceral regions, making up approximately 80 % of all adipose tissue in healthy subjects[9,10] (Fig. 2). Approximately one third of all cells in adipose tissue are adipocytes, with the rest represented by endothelial cells, macrophages, stromal cells, immune cells, and fibroblast, etc[10]. Human white adipocytes are spherical unilocular cells with a diameter of 50 to 200 μm and own a crescent shaped nucleus in the periphery of the cells and a unique large lipid droplet that takes up~90 % of the cytoplasm[11] (Fig. 2).

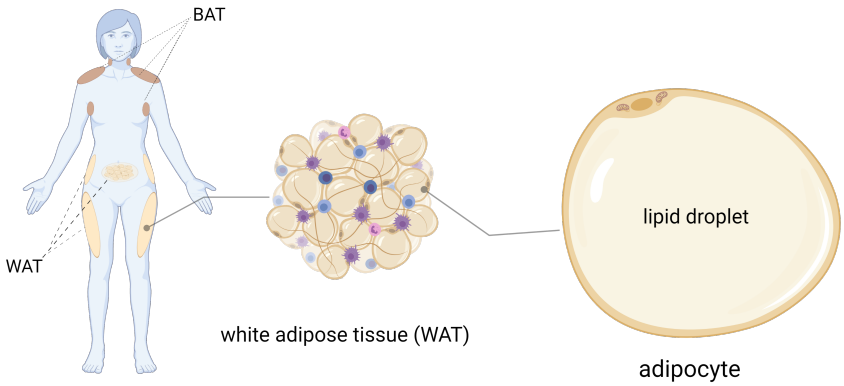

Figure 2. Schematic diagram of distribution and morphology of adipose tissue in the human body. White adipose tissue is mainly comprised of adipocytes, but also endothelial cells, macrophages, immune cells, and fibroblast. Created with BioRender.com.

To study the structure of human adipocytes and define accurate subcellular localization of interest of proteins in adipocytes, human abdominal subcutaneous adipose tissue was isolated and prepared into ultrathin sections and imaged by transmission electron microscopy (TEM). In contrast to adipocytes visualized by confocal microscopy, the thin lipid monolayer separating lipid droplet and cytoplasm, organelles in the cytoplasm, plasma membrane, exocytotic vesicles lining on the plasma membrane and basal laminar can clearly be seen by applying TEM (Fig. 3) (Paper I). Thus, TEM is suggested to be effective tool to investigate subcellular localization of proteins in human adipocytes.

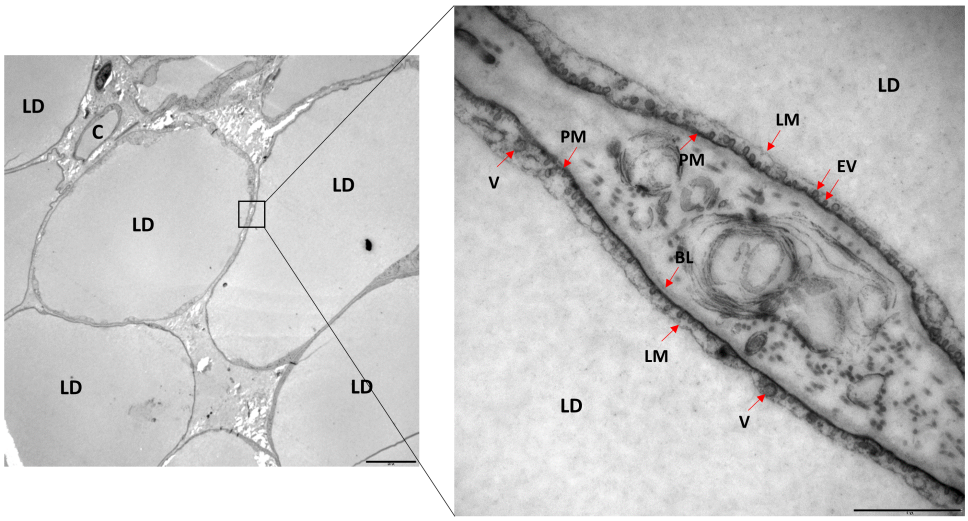

Figure 3. The microscopic visualization of human adipose tissue. The region highlighted by red box is zoomed in. LD, lipid droplet; C, capillary; LM, lipid monolayer; PM, plasma membrane; BL, basal laminar. V, vesicles in cytoplasm; EV, exocytotic vesicles. Scale bars, 20 μm (left) and 1 μm (right).

Glucose and lipid metabolism in adipocytes is fundamentally crucial to supply energy to other tissues and cells and maintain whole-body energy homeostasis[12]. Glucose ingested from the blood is metabolized by the pathway of glycolysis in adipocytes. Glycolysis is initialized by glucose transport across cell membrane into adipocytes, mediated by glucose transporters (GLUTs) residing in the plasma membrane. The lipid, mainly referring to triacylglycerol (TAG) is synthesized by glycerol-3-phosphate (Gro3P) and fatty acids through lipogenic pathway, while TAG is hydrolysed into glycerol and fatty acid upon lipolytic signal after fasting or exercise[13]. The glycerol hydrolysed from TAG is effluxed from adipocytes by aquaporins (AQPs), a family of membrane channels. Specifically, GLUT4 is a member of GLUT family expressed exclusively in adipocytes and muscle cells, whereas AQP7 is an aquaporin showing most abundant expression in human adipose tissue.

Glycolysis

Carbohydrate mainly including glucose, fructose and galactose are the major source of energy in the human body, in which glucose is a central molecule in the carbohydrate metabolism[14]. Glucose is metabolized by glycolysis in human adipocytes and other cells (Fig. 4), a biological process where glucose is converted into pyruvate following glucose uptake through cell membrane and glucose

phosphorylation, resulting in ATP production[15]. Simply described, glucose transported from the blood into cells is the initiating step for glycolysis, after which intracellular glucose is phosphorylated and converted into dihydroxyacetone-3-phosphate (DHAP) and glyceraldehyde-3-phosphate (G3P) by the synthesis of intermediates, fructose-6-phosphate and fructose-1,6-biphosphate. A significant proportion of DHAP is reduced to Gro3P by the catalysis of Gro3P dehydrogenase (GPD1), while GA3P is finally utilized for the production of pyruvate via stepwise catalytic reactions. Eventually, the pyruvate forms acetyl coenzyme (Acetyl-CoA) in aerobic conditions in mitochondria and enters tricarboxylic acid cycle (TCA cycle, also known as citric acid or Krebs cycle).

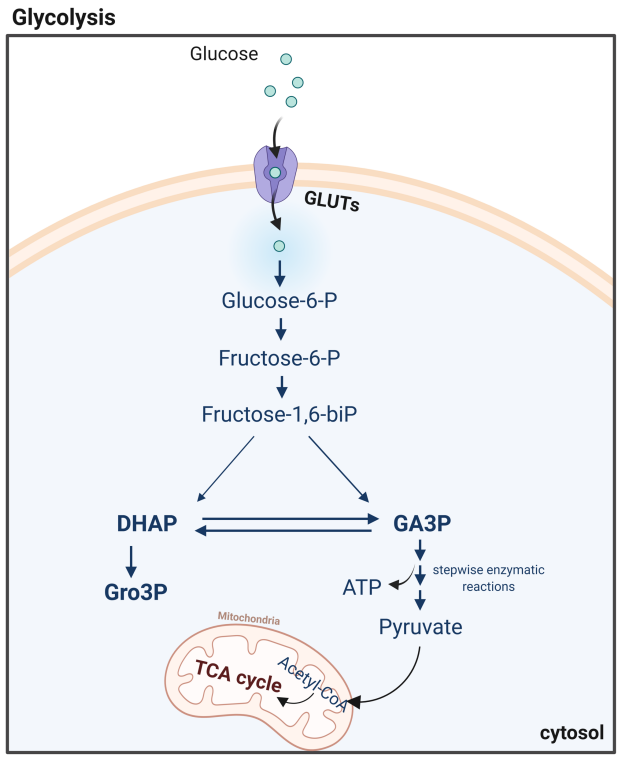

Figure 4. The simplified illustration of glycolysis pathway in human adipocyte. Created with BioRender.com.

Glucose transporters (GLUTs) in adipocytes

Glucose is a hydrophilic molecule that can only pass through the hydrophobic lipid membrane of cells by GLUTs. GLUTs are encoded by solute carrier family 2A genes (SLC2A) and are members of major facilitator superfamily (MFS) and facilitate the glucose transport along concentration gradient. Fourteen GLUTs have been identified in humans, and they are categorized into 3 classes according to their sequence similarity: class 1 (GLUTs 1–4, 14); Class 2 (GLUTs 5, 7, 9, and 11); and Class 3 (GLUTs 6, 8, 10, 12, and 13)[16], and show cell dependent distribution. Multiple GLUTs with different kinetics and regulatory properties are expressed in some cells and function in a coordinated manner to maintain homeostasis of glucose in physiological condition[17]. Herein, it's elucidated by transcriptome sequencing with three samples from one patient that *SLC2A1* (GLUT1), *SLC2A3* (GLUT3), *SLC2A4* (GLUT4), *SLC2A5* (GLUT5), *SLC2A6* (GLUT6) and *SLC2A8* (GLUT8) genes are expressed in significant level in human adipose tissue (Table 1). GLUT1, GLUT3 and GLUT4 belonging to class 1 are well-characterized, particularly GLUT4 is known as insulin-regulated glucose transporter expressed exclusively in the adipose tissue and muscle[18].

Table 1. The normalized GLUTs gene expression values of transcriptome sequencing.

Gene name	Sample 1	Sample 2	Sample 3
SLC2A1	84	67	61.4
SLC2A2	0	0	0
SLC2A3	7.9	7	6
SLC2A4	13	12	11
SLC2A5	100	96.5	94.5
SLC2A6	20	15.7	3
SLC2A7	0	0	0
SLC2A8	6.2	4.4	4.2
SLC2A9	1.7	2.2	1.4
SLC2A10	1.4	1.5	1
SLC2A11	2.8	2	0
SLC2A12	0	0	0
SLC2A13	2.7	2.2	0.8
SLC2A14	0	0	0

GLUT1

GLUT1, encoded by *SLC2A1* gene and comprised of 492 amino acids with molecular weight of 55 kDa, is the second most abundant GLUT in adipose tissue (Table 1). GLUT1 shows ubiquitous distribution nearly on all types of cells and mediate basal glucose uptake. Particularly, 5-10 % of total proteins on the membrane of human erythrocytes are GLUT1[19]. Additionally, it is also found in endothelial cells of blood-tissue barrier, indicating that GLUT1 has an important role in glucose supply to brain and other organs[20]. In insulin-sensitive cells, such as adipocytes and muscle cells, GLUT1 exists and mediates glucose uptake in association with GLUT4[21]. Due to the extensive distribution, indispensable physiological function, and its association with tumour cells development, GLUT1 has become a putative therapeutic target and prognostic indicator for cancer[22].

GLUT3

GLUT3 is an isoform of GLUTs predominantly expressed in adult brain, in addition, it's also distributed widely in human liver, kidney, placenta, and myocardium[23,24], and small amounts in adipose tissue (Table 1). Human GLUT3 consists of 496 residues and shares sequence identity of 64 % with GLUT1, and it has high affinity for glucose (Km ~1.5 mM)[25]. The ubiquitous distribution of GLUT3 in human tissues suggests that it is likely to be responsible for basal glucose transport together with GLUT1. GLUT1 is primarily responsible for glucose transport across the blood-brain barrier, while GLUT3 controls the uptake of glucose into neurons in brain[26]. GLUT1 and GLUT3 are overexpressed in tumours in which the demand of glucose increases dramatically because of the Warburg effect[27], which suggests GLUT3 to also be a potential target in cancer therapy. Transcriptome sequencing in our study indicates that GLUT3 mRNA is expressed in human white adipose tissue, which correlates well with the data provided by Human Protein Atlas (https://www.proteinatlas.org/).

GLUT4

GLUT4, an exclusive insulin-sensitive glucose transporter, is expressed primarily in adipose tissue (Table 1) and muscles[18]. A unique characteristic of GLUT4 is the insulin mediated translocation between cytoplasm and plasma membrane in adipocytes during glycolysis or increased energy demand, known as GLUT4 trafficking[18]. GLUT4 is primarily located at multiple intracellular compartments, such as trans-Golgi network (TGN), endosomes and GLUT4 storage vesicles

(GSV), and translocated and fused with plasma membrane by a complicated signaling pathway and trafficking machinery upon insulin stimulation, and thus mediating glucose uptake into cells[2,18,28]. GLUT4 is comprised of 509 amino acids, which presents the sequence identity of 64 % with GLUT1, and 56% with GLUT3, according to ClustalW.

Lipogenesis

Lipogenesis is a crucial process in the cell in which TAG is synthesized by glycerol (or glycerol-3-phosphate in adipocytes) and fatty acids (FAs). Most of lipogenesis takes place in hepatocytes, while TAG can be synthesized in adipocytes as main energy reserve from carbohydrate metabolism (Fig. 5A)[6]. Gro3P, either reduced from DHAP during glycolysis or produced from glyceroneogenesis during fasting or low carbohydrate intake, serves as a starting substrate[29], and thus being located at the intersection of glucose and lipid metabolism. Fatty acids as the other substrate used in the lipogenesis mainly originate from ingested fat and *de novo* TAG synthesis in adipocytes[30]. TAG synthesized in hepatocytes and ingested from intestine are transported to the capillary of adipose tissue in the form of very low-density lipoproteins (VLDLs) and chylomicrons (CM), respectively, in which they are hydrolysed by lipoprotein lipase (LPL) to release fatty acids[6]. Afterward, fatty acids are transported into adipocytes and esterified into acyl-CoA. Also, fatty acids utilized for lipogenesis are produced in the form of acyl-CoA from glucose via glycolysis in adipocytes (de novo TAG synthesis). Pyruvate is converted into citrate by TCA cycle in mitochondria during glycolysis, and then citrate is transported back to cytoplasm in which it is lysed into acetyl-CoA. Finally, acetyl-CoA as the basic backbone molecule is catalysed into fatty acyl-CoA by a series of enzymatic reactions.

Lipolysis

Lipolysis is a unique metabolic process occurring in adipocytes. Upon increased energy demands, such as after fasting or exercising, TAG is hydrolysed into glycerol and fatty acids, (Fig. 5B). The lipolysis pathway is catalysed by three main lipases: adipocyte triglyceride lipase (ATGL), hormone sensitive lipase (HSL) and monoacylglycerol lipase (MGL)[7], and tightly regulated by adrenergic signal, such as catecholamine stimulation. These three lipases function jointly to hydrolyse TAG sequentially and release three FAs. FAs released from lipolysis can be re-esterified into TAGs, in addition to functioning as signal molecules[31]. Likewise, hydrolysed

glycerol can also be re-esterified to TAGs by firstly forming Gro3P catalysed by the glycerol kinase (GK)[13,32]. However, only low level of GK is expressed in human adipocytes, in particular white adipocytes (WAT)[12], thereby ensuring that glycerol released from lipolysis is effluxed from adipocytes via aquaglyceroporins residing in the plasma membrane[12,33].

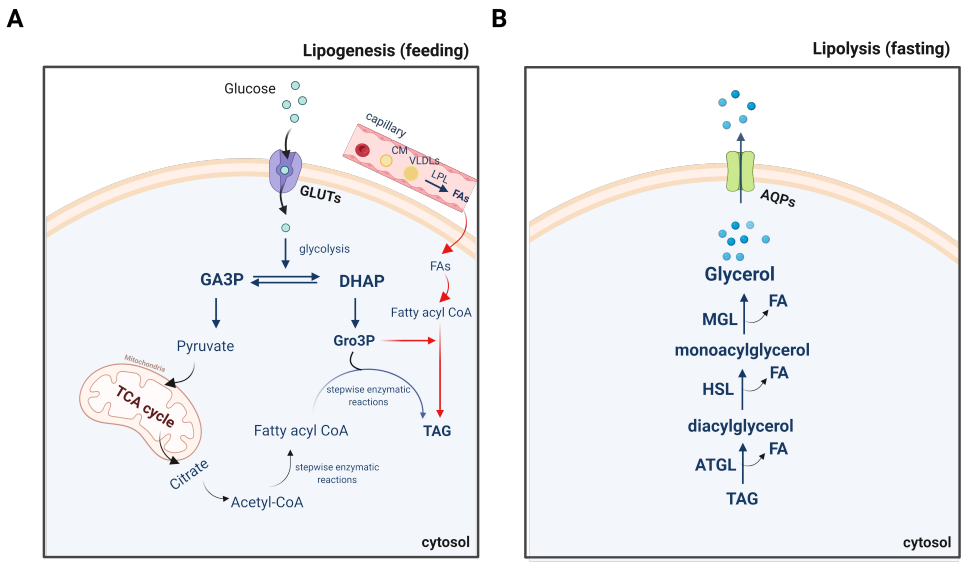

Figure 5. Simplified diagram of lipogenesis (A) and lipolysis (B) in human adipose tissue. With the uptake of excessive energy, TAG is synthesized by Gro3P and fatty acids in the form of fatty acyl CoA originating from glycolysis or ingested fat accumulated in capillary[6]. Upon increased energy demand, TAG is hydrolyzed into glycerol and free fatty acids by ATGL, HSL and MGL sequentially[7]. Created with BioRender.com.

Aquaporins (AQPs) in adipocytes

Aquaporins (AQPs) are membrane channels that facilitate the flux of small solutes, such as water and glycerol, etc., through cell plasma membrane to maintain osmotic balance and glycerol homeostasis. AQPs are usually divided into three groups: the orthodox aquaporins (water selective channels including AQP0, AQP1, AQP2, AQP4, AQP5, AQP6 and AQP8), aquaglyceroporin (AQP3, AQP7, AQP9 and AQP10, known as glycerol channels, also transport urea and arsenic trioxide) and the superaquaporins (AQP11 and AQP12) that may involve in water/glycerol transport of intracellular organelles[34]. AQP7 was the first identified glycerol channel in adipose tissue and controls glycerol efflux in adipocytes by trafficking from

cytoplasm to plasma membrane upon lipolysis signal[35,36], and later, other aquaglyceroporins including AQP3, AQP9 and AQP10 were also suggested to be expressed in adipocytes[37,38]. This correlates with our data of transcriptome sequencing and RT-PCR, in which *AQP7* showed significantly higher level of expression than other *AQPs* (Table 2 and Fig. 6) (Paper II). Interestingly, apart from aquaglyceroporins, *AQP1* as an orthodox aquaporin shows significant expression at the mRNA level (Table 2 and Fig. 6) (Paper II).

Table 2. The normalized AQPs gene expression values of transcriptome sequencing (Table 1 in Paper II).

Genes name	Sample 1	Sample 2	Sample 3
AQP1	11	8.5	11
AQP2	0	0	0
AQP3	9	3.4	2.6
AQP4	0	0	0
AQP5	0	0	0
AQP6	0	0	0
AQP7	120	118	115
AQP8	0	0	0
AQP9	12	11	9
AQP10	0	0	0
AQP11	1	1	1
AQP12	0	0	0

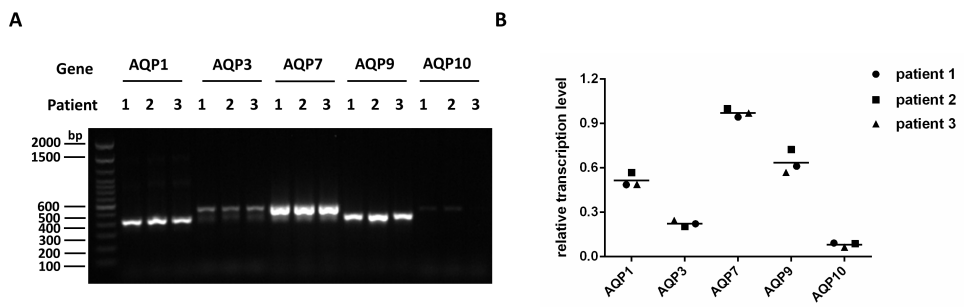

Figure 6. Gene expression analysis of AQPs in human primary adipocytes from three patients. (A) RT-PCR of different AQPs. (B) Relative transcriptional level analysis of AQPs (Figure 1 in Paper II).

AQP1

AQP1 was the first functionally identified member as water channel in AQP family in erythrocytes[39]. Later, AQP1 was also found in human apical and basolateral membranes of renal proximal tubules, ciliary body of the eye, the choroid plexus in the brain, microvascular structures of the respiratory system and the central nervous system[40]. To the best of our knowledge, AQP1 has not previously been identified in human white adipose tissue until our study (Paper II). Interestingly, previously hyperosmotic stress has been shown to suppress insulin signal in 3T3-L1 adipocytes, resulting in insulin-resistance mediated by phosphorylation of IRS-1 (insulin receptor substrate 1)[41]. Moreover, concentration-dependent upregulation of AQP1 expression has been suggested during hyperglycaemia in human aortic endothelial cells[42]. In addition, AQP1 has been shown to be relevant with hyperglycaemia-induced insulin resistance in endothelial cells[43]. Thus, we speculate that AQP1 may play a role to facilitate shuttling of water from adipocytes upon hyper-osmotic stress during hyperglycaemia (Paper II)[44]. In addition, AQP1 was suggested to be regulated by protein kinase C (PKC), relevant with phosphorylation of T157 at the intracellular loop and T239 at the C terminus[45] (Fig. 7).

AQP3

AQP3 belonging to aquaglyceroporin group is a membrane channel facilitating the permeation of water and glycerol[46]. AQP3 is expressed abundantly in basolateral plasma membranes of multiple human epithelia and keratinocytes of epidermis in human skin[47-50]. Thus, AQP3 was suggested initially to be a major participant in water regulation in skin barrier and osmotic homeostasis in the human body[49]. In addition, AQP3 expression was detected in human visceral and subcutaneous adipose tissue (Paper II) and regulated by insulin and leptin, in which AQP3, in analog to AQP7, may facilitate glycerol efflux from adipose tissue[51]. However, the concrete function of AQP3 in adipose tissue has not been clarified yet.

AQP7

AQP7 is abundantly expressed in human adipose tissue where it facilitates glycerol efflux across the plasma membrane. Experimental evidence indicates that AQP7 is expressed in both adipocytes and in the capillary endothelial cells in white adipose tissue[38]. AQP7 is translocated from the cytoplasmic compartment to the plasma membrane to efflux glycerol in response to adrenergic signal during lipolysis[35,38,51]. AQP7 consists of 342 amino acids, and in contrast to other AQPs expressed in human adipocytes it has long cytoplasmic termini (Fig. 7) (Paper II). PKA-phosphorylation sites (S10/T11) have been identified at N terminus of AQP7

(Fig. 7) (Paper II) and suggested to be important for regulating the AQP7 translocation in adipocytes[4].

AQP9

AQP9 was identified as a glycerol channel located on the plasma membrane of human and rat hepatocytes[52-54]. In addition to hepatocytes, AQP9 has also been reported to be expressed in human omental and subcutaneous adipocytes (Paper II), in which AQP9 expression on plasma membrane of human adipocytes was up regulated in response to insulin stimulation, adversely, downregulated upon leptin treatment, suggesting AQP9 might favour glycerol influx into adipocytes[51]. Interestingly, unlike AQP3 and AQP7 translocating from cytoplasmic compartments to plasma membrane in adipocytes upon hormone treatment, AQP9 is expressed consistently on the plasma membrane[51]. AQP9 owns a PKC phosphorylation site, the serine at position of 11 (Fig.7), which was shown previously to be important for membrane localization of AQP9[55].

AQP10

AQP10 was firstly identified as water and glycerol channel in the human small intestine, presenting high sequence identity with other aquaglyceroporins[56]. Recently, AQP10 was identified and showed permeability for both water and glycerol in human white adipose tissue[38]. Interestingly, AQP10, analogously to AQP7, appears to translocate between the surface of lipid droplet and the plasma membrane of adipocytes upon isoproterenol stimulation, thus representing an alternative pathway for glycerol efflux through plasma membrane of adipocytes[38]. Later it was suggested by the structural analysis that AQP10-mediated glycerol efflux in adipose tissue is regulated by pH-dependent gating mechanism[57]. In contrast, the data of both transcriptome sequencing and RT-PCR in our study showed that AQP10 is not expressed at mRNA level or at much lower level than other AQPs in human subcutaneous adipose tissue (Paper II), suggesting the expression level of AQP10 could be varied within the population.

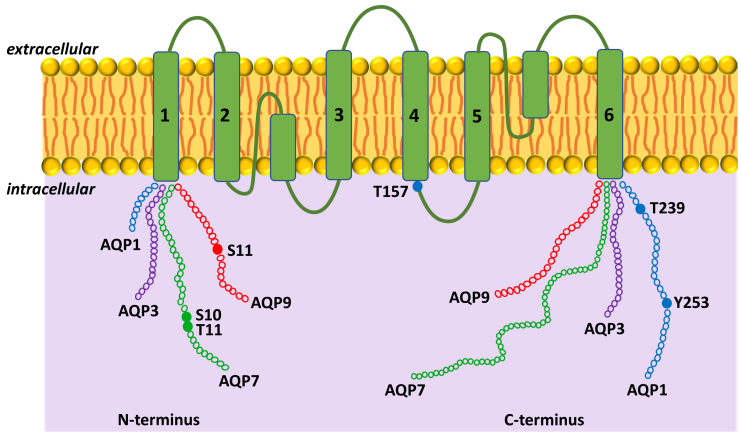

Figure 7. Topological representation and phosphorylation sites of AQPs expressed in human adipocytes. The termini of AQPs are marked as continuous circles while phosphorylation sites are highlighted as filled circles (Figure 2C in Paper II).

Protein and protein interaction important for the regulation of GLUT4 and AQP7/3 trafficking

Protein and protein interactions (PPIs) play a fundamental role in most biological processes in human body, including gene expression, protein localization, signal transduction, nutrient metabolism, and energy homeostasis, etc[58]. PPIs are also crucial in the regulation of membrane proteins, and thus affecting relevant metabolic pathways. Several proteins interacting with GLUTs and AQPs have been identified, including (but not limited to) GLUT4 and TUG (tether containing ubiquitin domain for GLUT4 in mouse)[59], GLUT1 /GLUT4 /GLUT5 and TXNIP (thioredoxin-binding protein)[60,61], AQP7 and PLIN1 (perilipin 1)[4], AQP0 and CaM (calmodulin)[62], AQP2 and LIP5 (lysosomal trafficking regulator–interacting protein 5)[63], AQP5 and PIP (prolactin-inducible protein)[64]. The regulation of the trafficking of GLUT4 and AQP7 are complicated biological processes in cells, here I will focus on TUG and PLIN1, representing important regulating factors for GLUT4 and AQP7, respectively.

ASPL

ASPL encoded by alveolar soft part sarcoma chromosomal region candidate gene 1 (ASPSCR1) with C terminal ubiquitin domain (UBX) is the human homolog of TUG[65,66], where TUG is a tether containing ubiquitin domain for GLUT4 in mouse[59]. TUG has 75 % sequence identity with ASPL. So far, the structural

information of full-length ASPL is not known, however the C-terminal domain containing UBX has been determined by X-ray crystallography in complex with another protein (p97) (PDB ID: 5IFS)[67]. To generate a three-dimension model of full-length ASPL, AlphaFold was applied[68], showing that ASPL has two N-terminal ubiquitin like (UBL) domains, in addition to the C-terminal UBX, while the remaining protein is likely to be unordered (Fig. 8) (Paper I). The UBX domain in ASPL exhibits canonical ubiquitin-like β grasp folding (β β α β β) (Fig. 8) (Paper I), possibly related with ubiquitination process or protein interaction[65,67,69].

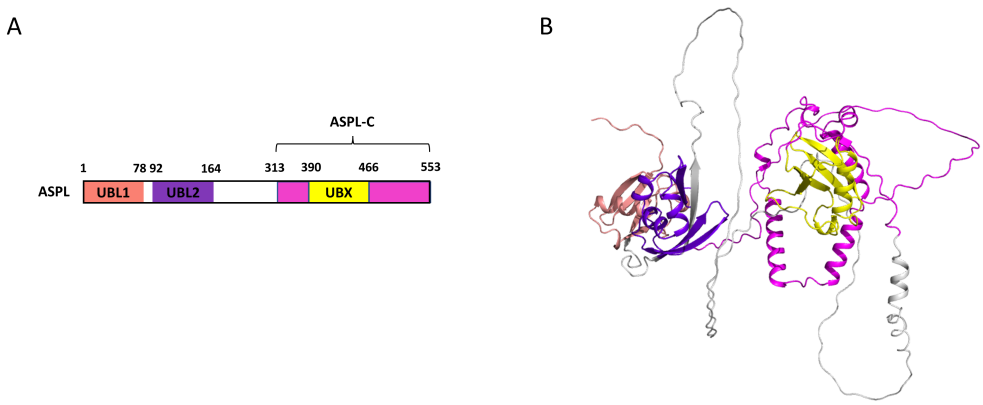

Figure 8. Human ASPL structure predicted by AlphaFold (A) and schematic representation (B). The ASPL structure is shown as cartoon and colored by domains (Figures 1C-D in Paper I).

Insulin-regulated GLUT4 trafficking is a complicated process involving multiple recycling steps and signalling pathways[28]. In 3T3-L1 cells (mouse adipose cell line), TUG sequesters GSVs intracellularly by utilizing its N-terminal ubiquitin domain to bind with intracellular domain of GLUT4 in the absence of insulin. Upon insulin stimulation, it is cleaved and thus releasing the GSVs to be translocated to plasma membrane to mediate glucose uptake[1,59,70] (Fig. 9). However, if similar mechanism takes place in humans, is unknown.

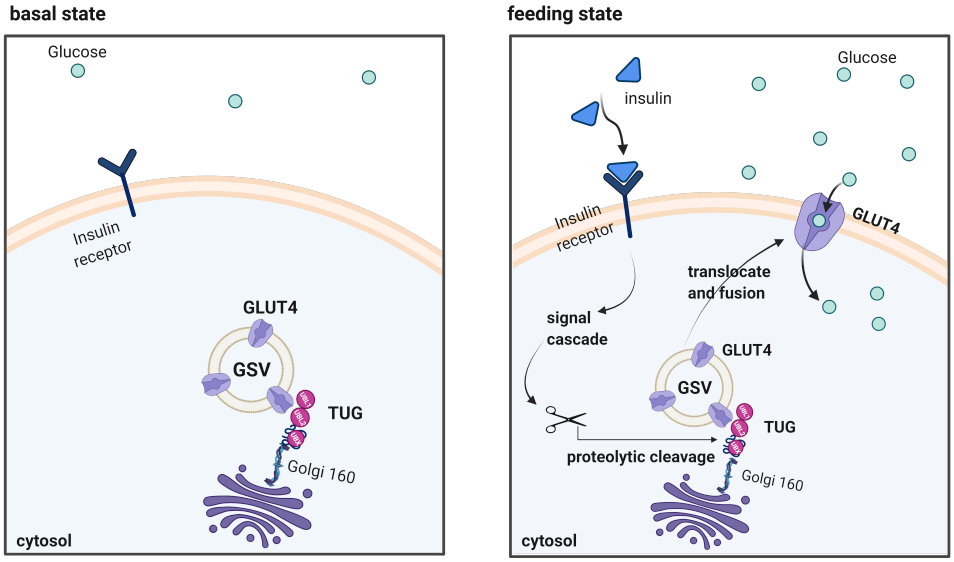

Figure 9. TUG mediated GLUT4 trafficking in mouse adipose tissue (3T3-L1)[1,2]. In basal state, GLUT4 forms complex with TUG, sequestered on Golgi apparatus by Golgi 160. The complex of GLUT4 and TUG is broken by the proteolytic cleavage upon insulin stimulation, thus GLUT4 is released and translocated to plasma membrane to mediate glucose uptake. Created with BioRender.com.

GLUT4 interaction with ASPL (Paper I)

To resolve if ASPL can play a similar role in humans as TUG does in mouse, the interaction between GLUT4 and ASPL was studied applying a combination of biochemistry and biophysics (Fig. 10). Firstly, wild type GLUT4 showed to bind with ASPL in pull down assay (Fig. 10A). To clarify what parts of GLUT4 are contributing to the interaction, far dot western blot was applied and suggested that the C-terminal domain of ASPL binds with GLUT4 (Fig. 10B). By performing surface plasma resonance (SPR) and cross-linking mass spectrometry (XL-MS), we could show that GLUT4 can form a complex with ASPL utilizing its intracellular helical bundle (ICH) to bind the C terminus of ASPL (Figs. 10C-D). This indicates that ASPL may regulate GLUT4 trafficking in human in a similar manner as in rodents but using additional domains.

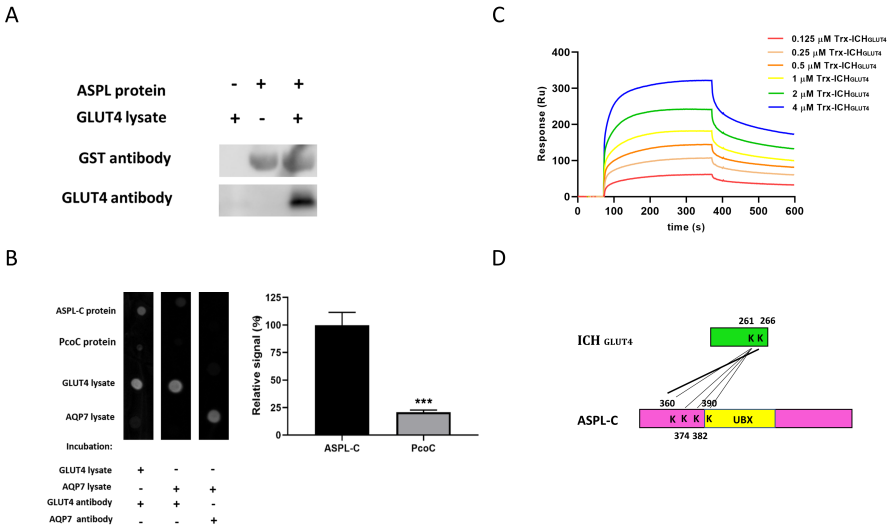

Figure 10. The interaction study in vitro of GLUT4 and ASPL. (A) Pull-down analysis. (B) Representative far dot western blot and quantification analysis. (C) The interaction analysis by surface plasma resonance (SPR). (D) Schematic diagram of crosslinking sites between ICHGLUT4 and ASPL-C (Paper I).

Perilipin 1 (PLIN1)

Perilipins (PLINs) are lipid droplet associated proteins and include mainly five members (PLIN1-5)[71]. PLIN1 is expressed exclusively on the outer surface of lipid droplet in adipocytes and consists of an N-terminal PAT domain, an amphipathic 11-mer repeat, a central 4-helix bundle, and a unique long C-terminal domain (Fig. 11) (Paper II). The 11-mer repeat is conserved through all PLINs and has been presented to be a key domain mediating lipid droplet targeting of PLIN1[72]. In addition to 11-mer repeat, the 4-helix bundle appears to be important for PLIN1 anchoring on the lipid droplet, while the C-terminal domain has been reported to bind with ABDH5 (ATGL co-activator AB-hydrolase-containing 5), and thus suppressing the activity of ATGL[73].

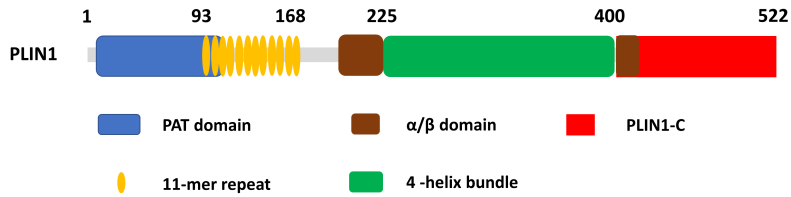

Figure 11. Schematic representation of PLIN1 (Figure. 3A in Paper II).

It has been reported that PLIN1 serves as a crucial regulator in lipolysis by forming docking sites on the lipid droplet and interacting with HSL upon protein kinase A (PKA) mediated phosphorylation[3,5,11] (Fig. 12). Additionally, PLIN1 is suggested to regulate the activity of ATGL by releasing ABHD5 upon PKA activation, and thus regulating lipolysis[74] (Fig. 12). Interestingly, AQPs are known to be regulated via a protein-protein interaction network tightly associated with phosphorylation levels[75]. Specifically, PKA mediated phosphorylation releases AQP7 from PLIN1 by inhibiting the interaction, and thus likely facilitating AQP7 translocation to plasma membrane to mediate glycerol efflux[4] (Fig. 12). The termini of AQP7 have been shown to be important for the interaction with PLIN1[4], however, which domains of PLIN1 contributing the interaction remains unclear.

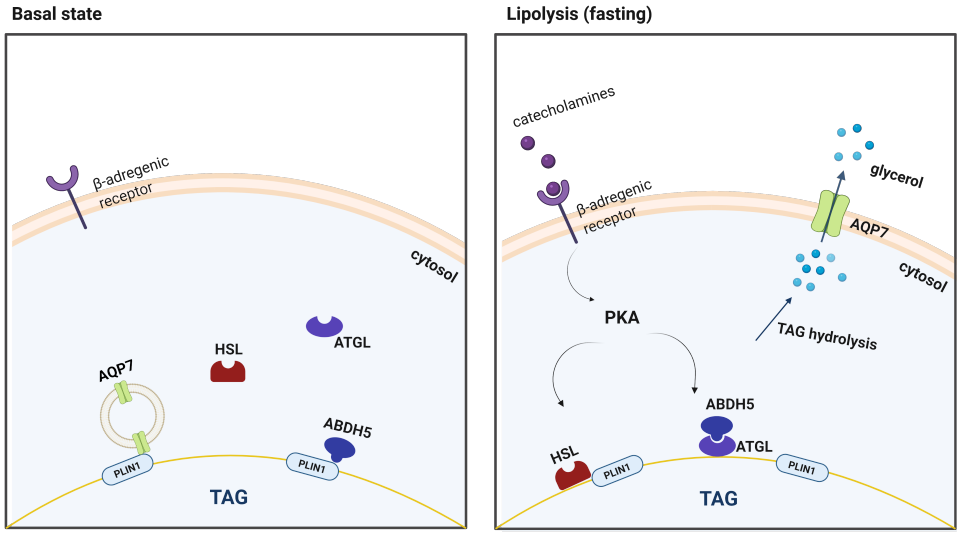

Figure 12. Simplified diagram of lipolysis regulation mediated by PLIN1. In basal state, PLIN1 forms complex with AQP7 and ABDH5, respectively, and HSL is separated from lipid droplet[3,4]. Upon PKA activation, PLIN1 releases ABDH5 and AQP7, thus activating ATGL and facilitating the trafficking of AQP7, respectively, and creates docking sites on the surface of lipid droplet for HSL[3,5]. Created with BioRender.com.

AQP3 and AQP7 interacting with PLIN1 (Paper II)

To find which domains of PLIN1 that are important for complex formation with AQP7, PLIN1 was subjected to hydrophobicity analysis using hydropathy scale. Clearly, the long C-terminal domain from residue 400 to 522 (PLIN1-C) presents hydrophilic characteristic, while the remaining parts of PLIN1 are hydrophobic, suggesting that the C-terminus may be exposed to the hydrophilic cytoplasm (Fig. 13A). Thereby, PLIN1-C was produced heterologously in *E.coli* and its binding with AQP7 in vitro was confirmed by BN-PAGE (Fig. 13B). Furthermore, far dot western blot approach was applied to investigate potential complex formation between PLIN1 and other AQPs expressed in adipocytes. This suggested that AQP3 also can form a complex with PLIN1-C, in addition to AQP7 (Fig. 13C). Previously it has been shown that PKA activation attenuates complex formation between AQP7 and PLIN1 by phosphorylating N-terminus of AQP7, however, no PKA sites were identified in AQP3 (Fig. 7), indicating additional signalling pathways may control the property of AQP3, although AQP3 and AQP7 still may have partly redundant roles in adipocytes during lipolysis.

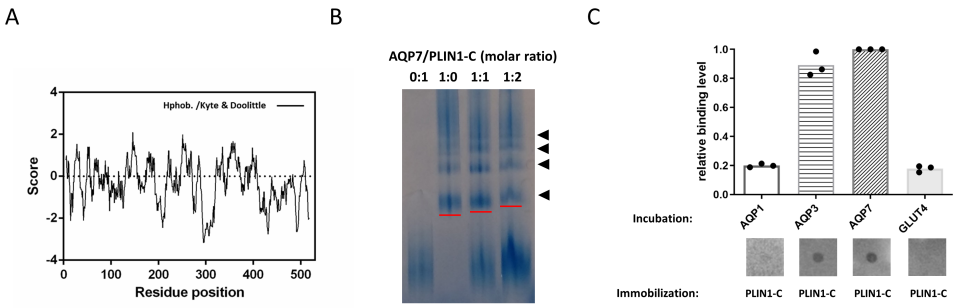

Figure 13. The interaction between PLIN1 and AQPs. (A) Hydrophobicity plot of PLIN1. (B) BN-PAGE of AQP7 and PLIN1-C in different molar ratios. (C) Representative far dot western blot and quantification with immobilized PLIN1-C protein, incubated with different AQPs lysate or GLUT4 lysate, respectively, Figures in Paper II.

Structural characteristics of GLUTs in human adipocytes

GLUTs are membrane uniporters facilitating sugar transport down the concentration gradient. Transcriptome sequencing in my work suggested that GLUT1, GLUT3 and GLUT4 are expressed at mRNA level in human adipose tissue. Specifically, GLUT4 is expressed exclusively in adipocytes and muscle cells and regulated by insulin. Herein, common structural folding of GLUTs was introduced according to structurally available GLUTs, and the study towards GLUT4 structure was initiated by producing recombinant protein of GLUT4 firstly, and complex model of GLUT4 and ASPL was proposed based on the study of protein and protein interaction.

Common structural features of human GLUTs

Structural information of human GLUT1 and GLUT3 and rat/bovine GLUT5 has been revealed by X-ray crystallography, suggesting that GLUTs own considerably conserved structural characteristic, consisting of two pseudo-symmetrical six-transmembrane helical domains at the N and C termini, connected by intracellular helical bundle (ICH)[76-78] (Fig. 14). The ligand (glucose/fructose) is bound in the central cavity located at halfway of transporting pathway (Fig. 14A) and transported through GLUTs by alternating access mechanism[76,77]. The N-terminal domain keeps stable relatively in the transport cycle, while the C-terminal domains undergo conformational fine-tuning around shuttling pathway to achieve substrate binding and release. Based on the structures of GLUT1 and GLUT3 as well as the development in protein structure prediction program[68], a computational GLUT4 model was generated using AlphaFold (Fig. 14B) (Paper I). Generally, GLUT4 exhibits the typical GLUT-fold with twelve transmembrane helices spanning the plasma membrane and intracellular helical domain (ICH), in addition, two cytosolic termini (N-term and C-term) that may be involved in GLUT4 trafficking[26]. Interestingly, the ICH domain in GLUT1 was suggested to serve as a door latch to coordinate the closure of intracellular gate and stabilize outward-facing conformation of GLUT1 by forming inner salt-bridge network and another salt-bridge with transmembrane domains[76]. Although GLUT4 structure can be simulated computationally, structure determination of GLUT4 is urgent to shed light on

glucose transporting mechanism and insulin mediated regulation of GLUT4 trafficking in human adipocytes.

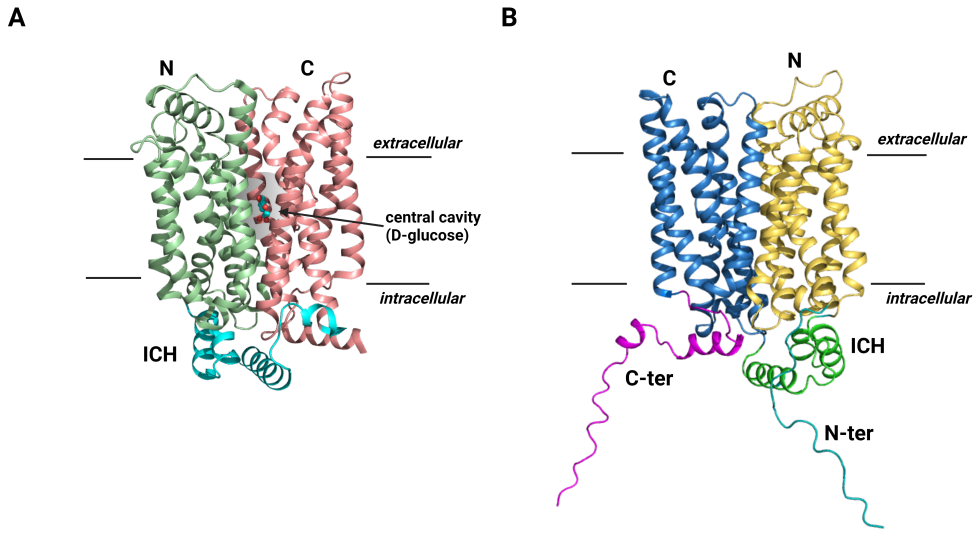

Figure 14. Structural characteristic of human GLUTs. (A) Human GLUT3 crystal structure (PDB ID: 4ZW9). N, C and ICH domains are marked by different colors. D-glucose is shown as sphere and central cavity is represented by gray shadow. (B) Human GLUT4 structure predicted by AlphaFold. The structure is shown as cartoon and colored by fragments. N-term and C-term represent cytoplasmic N and C termini, respectively (Adapted from Figure 1A in Paper I).

Towards GLUT4 structure

GLUT4 is a main glucose transporter in human adipocytes. To determine the structural information of GLUT4, recombinant protein was produced heterologously in *Pichia pastoris* and purified in the detergent. The AlphaFold model suggested that ICH is a cytoplasmic domain connecting two tandem transmembrane helical bundles (Fig. 14B) and has also been shown to bind to TUG involved in the regulation of GLUT4 trafficking in adipocytes[59]. As described above, ICH domain of GLUT4 was suggested to bind with ASPL-C. Here, the putative complex models of GLUT4 and ASPL were simulated by applying distance constrains below 33 Å on the domains of ICH and ASPL-C.

GLUT4 expression and purification

To facilitate structural analyses of GLUT4, we set out to produce homogeneous and pure recombinant protein. Firstly, rat GLUT4 (that shows 95 % sequence identity with human GLUT4) was fused N terminally with a His-tag and expressed heterologously in *Pichia pastoris*, and the membranes were prepared and solubilized in detergent. To isolate GLUT4 from yeast membranes effectively, detergent screening was performed by solubilizing membranes in Fos-Choline-12, CYMAL-6, LMNG, DM and DDM, with or without cholesteryl hemisuccinate tris salt (CHS). The efficiency of membrane solubilization was judged by western blotting, resulting in best solubilization properties of DM, in addition to Fos-Choline-12 (Fig. 15A). As Fos-Choline detergents may lead to destabilization of unfolding of membrane proteins[79], DM was selected for membrane solubilization to extract GLUT4 and the solubilization condition was further optimized by varying detergent concentration, solubilization time and temperature (Fig. 15B). Finally, GLUT4 was extracted from yeast membrane by 2 % DM at room temperature for 1 h followed by purification applying affinity chromatography (Fig. 15C). The protein identity was confirmed by Coomassie-stained SDS-PAGE and liquid chromatography-mass spectrometry (LC-MS). Afterwards, the protein was further polished by size exclusion chromatography (SEC) (Fig. 15D). Unfortunately, purified GLUT4 did not show good homogeneity upon SEC, suggesting that the protein was partly aggregated (Fig. 15D). Still, the protein eluted at the volume of approximate 13 mL in SEC showed single-particle distribution in negative staining (Fig. 15E), which paves the way for future sample optimization for structural study by single particle cryo-EM.

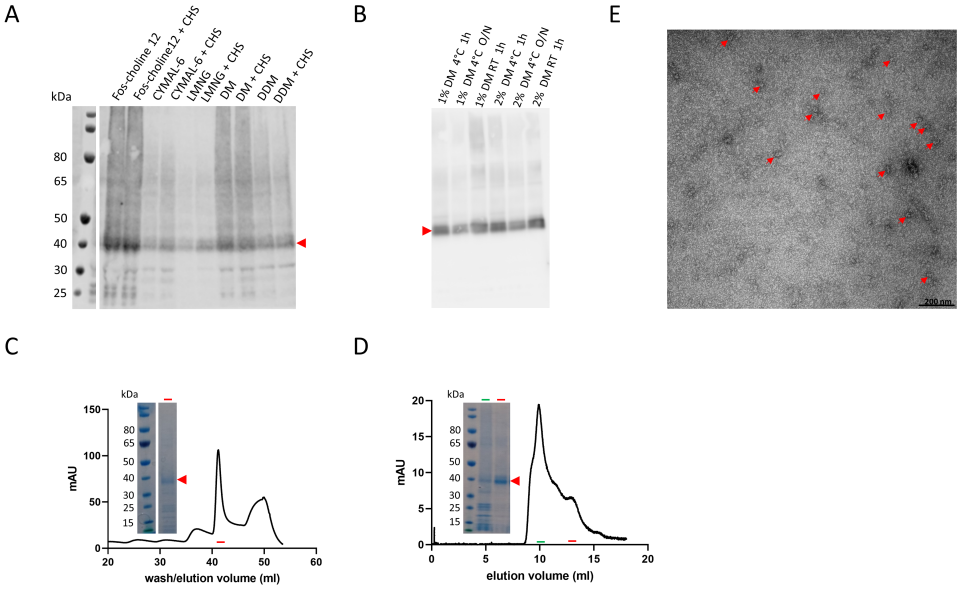

Figure 15. Rat GLUT4 expression in *Pichia pastoris* and initial purification trial. (A) Detergent screening to isolate GLUT4 from yeast membrane evaluated by western blotting stained with specific GLUT4 antibody. GLUT4 bands are marked by red arrow. (B) The optimization of membrane solubilizing condition via DM. The membrane solubilization was detected by western blot stained with specific GLUT4 antibody. GLUT4 bands are marked by red arrow. O/N, overnight; RT, room temperature. (C) GLUT4 was solubilized by DM and purified utilizing affinity chromatography. GLUT4 was identified by Coomassie stained SDS-PAGE and marked by red arrow. (D) GLUT4 sample from affinity chromatography was further purified by SEC (Superdex 200 increase 10/300 GL column). Different fractions from the peak labeled with short green and red lines, respectively, were detected by Coomassie stained SDS-PAGE. GLUT4 bands are marked by red arrow in SDS-PAGE. (E) Negative staining of GLUT4 protein. GLUT4 sample from figure D labeled with red line was stained with uranyl acetate and inspected by 200 kV TEM. The representative GLUT4 particles are highlighted by red arrow. The scale bar represents 200 nm.

The docking model of ICH_{GLUT4} in complex with ASPL-C

Global docking was performed for ICH_{GLUT4} and ASPL-C by constraining distance below 33 Å for each pair of identified crosslinking residues, generating five potential complex models. One of them was excluded as it sterically clashed with transmembrane domains of GLUT4. Remaining four models presented different binding modes with the ICH domain of GLUT4 being closed to either the UBX, the UBL2, or/and the N terminus of ASPL-C. Previously, UBL2 domain in TUG was suggested to be crucial to bind with GLUT4 in rodents[1,59], and combined the data of protein interaction we described above, we suggest that GLUT4 can form complex with ASPL by using its ICH domain to bind with both UBL2 and UBX domains in ASPL.

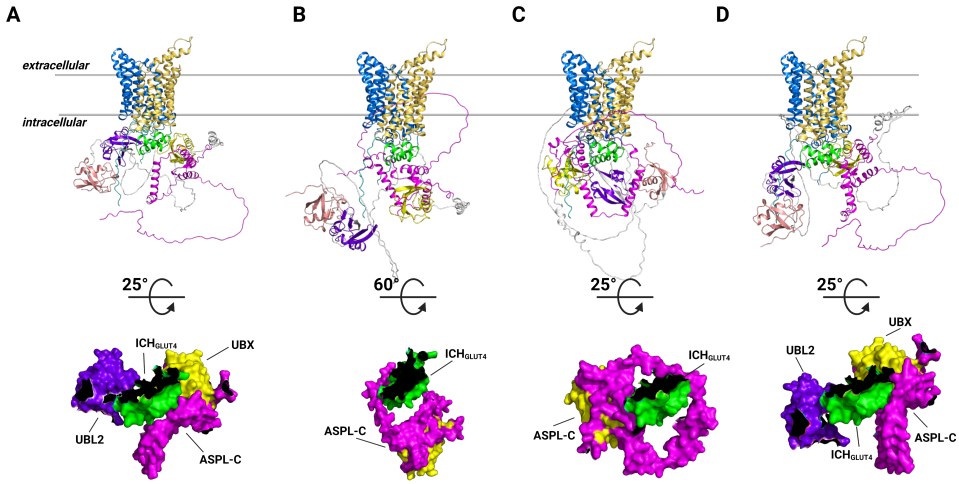

Figure 16. Docking models of GLUT4 and ASPL. Four potential models (A-D) were generated from global docking. ASPL and GLUT4 were colored with same schemes as figure 8 and 14B, and interaction interfaces between GLUT4 and ASPL were shown as surface, including ICHGLUT4 (green), UBL2 (purple blue), UBX (yellow) and N terminus of ASPL-C (magenta).

GLUT1 inhibitor (Paper III)

Cancer cells have increased glucose demands to maintain their rapid growth and proliferation than normal tissue, known as the Warburg effect[27,80]. It has been discovered that a vast majority of cancers and isolated tumour cell lines overexpress GLUT family members to satisfy the increased glucose demand[27,80,81]. Due to wide distribution and physiological importance in human tissues, GLUT1 is becoming an effective indicator in oncology diagnosis and prognosis[82], thereby GLUT1 inhibitors blocking the process of glycolysis and thus cell viability are being considered as a new promising cancer therapy[22]. In recent years, some small molecules have gained interest, such as STF31 and WZB117, however, their limited blocking ability to GLUT1 and controversial selectivity of inhibition has hindered further development into the clinic[83,84]. So far, the most promising candidate inhibitor is BAY-876 with high selectivity for GLUT1, instead of GLUT2/GLUT3/GLUT4[85]. However, at present, there is no available data to confirm its inhibiting effect *in vivo*. With the disclosure of GLUT-structures, more inhibitors have been designed based on structures and computational simulations. A series of salicylketoxime derivatives (PGLs) were developed as GLUT1 inhibitors and presented effective inhibition of glucose uptake and antiproliferative effect in lung cancer cells[86]. In our study, a significant decrease in glucose uptake was shown for PGL13 and PGL14 in giant vesicle assay (Fig. 17A). Subsequently, docking models of PGL14 and GLUT1 were generated, and the reliability of the models were assessed by molecule dynamic (MD) simulation. The overall analysis suggests that PGL14 may interact with the intracellular domain of GLUT1 in the partially occluded inward-facing conformation, in addition to binding to the central substrate site of GLUT1 in inward open conformation (Figs. 17B). Provided that GLUT1 shows the property of intrinsic tryptophan quenching upon ligand binding[87,88], a tryptophan quenching assay of GLUT1 upon addition of PGL13 and PGL14 was performed. Clearly, the intensity of fluorescence decreased gradually upon increasing concentrations of PGLs, whereas a right shift in the emission spectra and an increase of fluorescence intensity were observed at very high inhibitor concentrations (Figs. 17C-D). This is interpreted because of PGLs binding at two sites, both transmembrane and intracellular domains, but with different affinities, based on the models generated from docking and MD simulation (Figs. 17B-D). Combined with the data of PGLs effect in cell biological assays, we conclude that the PGL series of compounds are promising for the development of potential sensitizers for chemotherapy in AML therapy (Paper III).

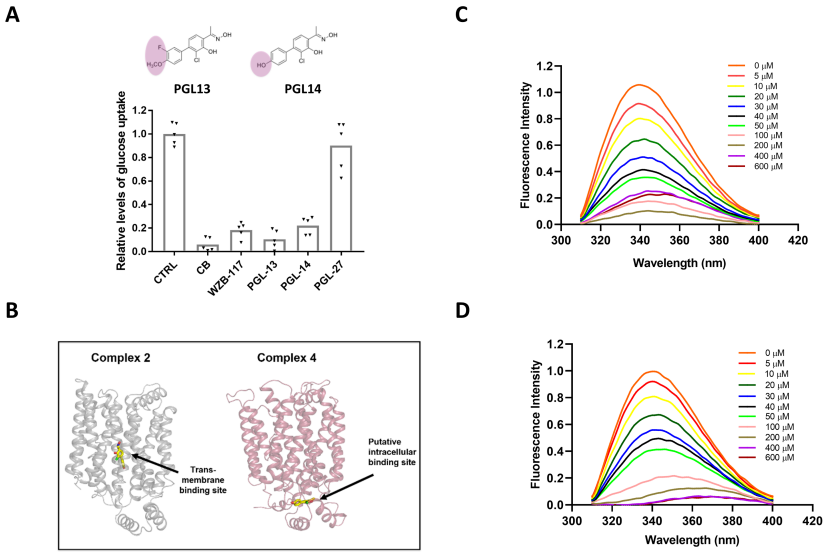

Figure 17. Inhibition of glucose uptake via GLUT1 by PGL compounds. (A) Inhibition of glucose uptake by inhibitors measured in giant vesicles. (B) Simulated models of PGL14 in complex with GLUT1. Complex 2 shows PGL14 binds at transmembrane domain of GLUT1, while complex 4 represents a model of PGL14 binding at intracellular domain in GLUT1. (C-D) Intrinsic tryptophan fluorescence quenching spectra of purified GLUT1 upon different concentrations of PGL-13 (C) and PGL-14 (D), with excitation wavelength at 295 nm (Adapted figure 1 in Paper III).

Structural characteristic of AQPs in human adipocytes

AQPs are a family of integral membrane protein permeating water/glycerol and/or other small solutes (urea and arsenic trioxide) across cell membrane. AQPs are mainly classified into aquaporins (selective permeation to water) and aquaglyceroporins (transport glycerol as well as urea and arsenic trioxide). To date, all available structures of human AQPs have been determined by crystallography, including AQP1[89], AQP2[90], AQP4[91], AQP5[92], AQP7[36] and AQP10[57].

Common structural features of human AQPs

AQPs are conserved structurally and adopt canonical AQP-fold consisting of six transmembrane helices (1-6) connected by five loops (A-E), two half helices (HX1 and HX2) dipping into the membrane and creating a pseudo seventh helix, a conserved Asn-Pro-Ala (NPA) motif, an aromatic/arginine (ar/R) pore constriction region known as the selectivity filter and two cytoplasmic termini (Figs. 18A-B). The NPA motif in combination with the selective filter at the extracellular vestibule, leads to selective permeation for either water or other solutes, such as glycerol, but exclusion of ions and protons[36,89,93]. In addition, the non-transmembrane loops and cytoplasmic termini are suggested to be important for gating[92,94], trafficking regulation[4,95], tetrameric stabilization[89] and interaction with other regulatory proteins[4,63,64]. AQPs favour to form tetramers (Fig. 18C), although each monomer functions independently as conducting channel for water or glycerol. However, the physiological function in details of the AQP-tetramer formation needs to be further clarified. In contrast to orthodox aquaporins, aquaglyceroporins are known to have wider and amphipathic selective filter, and thus selectively permeate glycerol across the membrane[31,89]. However, the residues comprising the selective filter are partly conserved among aquaglyceroporins (Fig. 18D), thus may result in their difference on the mechanism of selective permeation. Interestingly, AQP10 lack an aromatic residue at the selective filter, thereby presenting different selective property compared to AQP7[57]. AQP7, on the other hand, features an unusual NPA motif consisting of NAA (Asn-Ala-Ala) and NPS (Asn-Pro-Ser), thus missing the proline-proline stacking interaction of two half helices presented in nearly all AOPs[36,96] (Fig.

18B). Additionally, AQP7 has extended cytoplasmic termini suggested to involved in the regulation of AQP7 translocation in adipocytes (Fig. 18D).

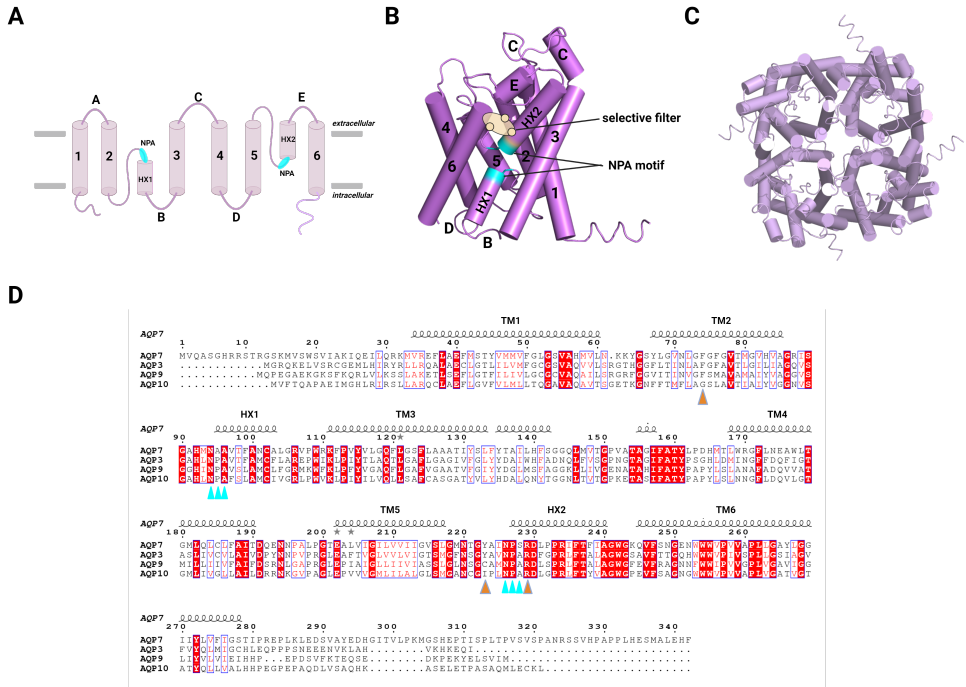

Figure 18. Structural characteristic of AQPs. (A) Topological representation of AQPs. NPA motif is highlighted as cyan oval. (B) A monomer of AQP7 cryo-EM structure (Paper IV). The NPA motif is colored in cyan and selective filter is marked as wheat oval. (C) A tetramer of AQP7 cryo-EM structure (Paper IV). The model is shown as cylinder from intracellular view. (D) Sequence alignment of aquaglyceroporins. Residues involving in selective filter and NPA motif are marked by wheat and cyan triangles, respectively.

Structurally determined human aquaglyceroporins

The structure of AQP7 at resolution of 1.9 Å was determined by X-ray crystallography (PDB ID: 6QZI)[36]. A glycerol conducting mechanism was proposed by the analysis of AQP7 crystal structure, suggesting the glycerol passes through the channel in a manner of part rotation by altering H-bond network[36]. AQP10 structural information (PDB ID: 6F7H) revealed by X-ray crystallography shows that AQP10 has wide selective filter and glycerol flux through the channel is regulated by a pH gate located at cytoplasmic side[57]. Although glycerol conducting mechanism was well elucidated from structures, both AQP7 and AQP10 lack termini and are affected by crystal packing. Still, two termini of AQP7 have been

suggested to be important for its trafficking in adipocytes[4]. Hence, to elucidate the structural properties of AQP7 in a non-crystallographic setting, as well as to reveal the structural information of full-length AQP7 with termini, AQP7 was subjected to the study of single particle cryo-EM (Paper IV).

AQP7 cryo-EM structure adopting the formation of dimer of tetramers (Paper IV)

To analyse the structure of full length AQP7 in a non-crystallographic setting, human AQP7 was expressed in *Pichia pastoris* and purified in GDN detergent before single particle cryo-EM data was collected and processed. The AQP7 structure adopted the formation of dimer of tetramers and was resolved to 2.55 Å with D4 symmetry and 3.0 Å without applied symmetry (C1). The final maps presented a double-layer density corresponding to two AQP7 tetramers, with the dimensions of approximately 10 nm in height and 6 nm in diameter (Fig. 19A). Clearly, the two AQP7 tetramers interact with each other by the protruding extracellular loop C from all eight monomers, forming compact octamer (Fig. 19B). Moreover, the central pore is formed by four independent monomers along the central axis (Fig. 19A-B).

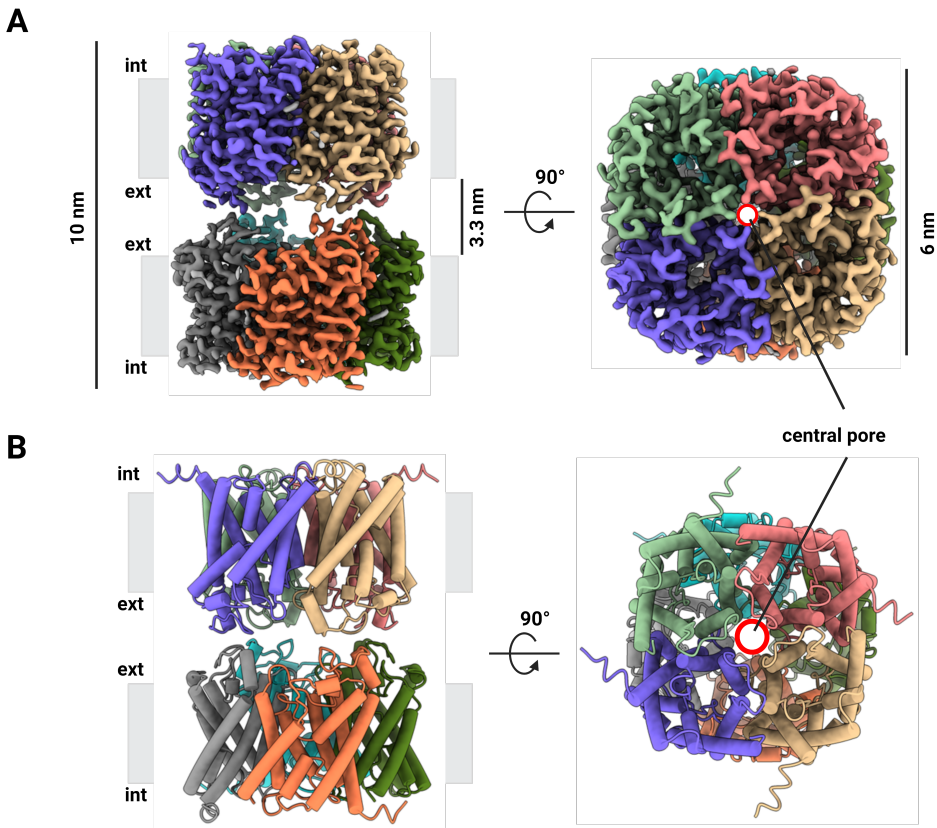

Figure 19. The overall structure of human AQP7 adopting dimer of tetramers determined by cryo-EM. (A) AQP7 cryo-EM map without symmetry application (C1) at the resolution of 3.0 Å viewed from side (left) and top (right). The map is colored by zone, and central pore is represented as red circle. (B) The model side (left) and top (right) views of AQP7 dimer of tetramers built from the map in figure A (Adapted from figures 1A-B in Paper IV).

Unique extracellular loop C in AQP7 cryo-EM structure

The human aquaglyceroporins, including AQP7, have an extended extracellular loop C between transmembrane domain 3 and 4 compared to the orthodox aquaporins (Figs. 20A and C). The opposing two tetramers in AQP7 cryo-EM structure pack each other by hydrophobic interactions of P151 and V152 in loop C within a distance of 4 Å, suggesting P151 and V152 are crucial for the formation of AQP7 dimer of tetramers (Fig. 20B). Although the loop C is a partly conserved structure among human aquaglyceroporins, P151 and V152 are not conserved, implying the dimer formation may be unique for AQP7 (Fig. 20C).

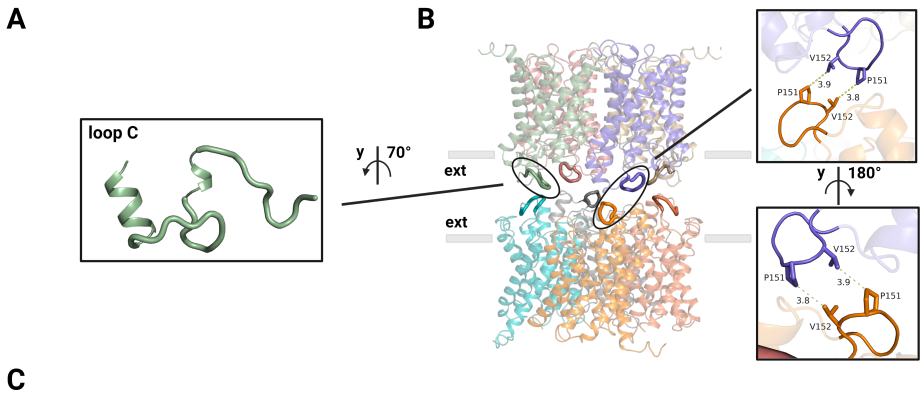

C

AQP7	FYTAILHFSGGQLMVTG**PV**A---TAGIFATYLPDHMT	167
AQP3	YYDAIWHFADNQLFVSG**PN**G---TAGIFATYPSGHLD	156
AQP9	YYDGLMSFAGGKLLIVG**EN**A---TAHIFATYPAPYLS	157
AQP10	YHDALQNYTGGNLTVTG**PK**E---TASIFATYPAPYLS	155

Figure 20. The loop C mediated stabilization of AQP7 dimer of tetramers. (A) Extracellular loop C shown as cartoon. (B) The model of AQP7 dimer of tetramers. The loop C in all monomers is shown as tubes. P151 and V152 are marked and the distance between them is shown in right zoom-in figures. (C) The sequence alignment of loop C among aquaglyceroporins (Adapted from figures 3A-C in Paper IV).

The comparison between crystal and cryo-EM structures of AQP7

The crystal structures reveal the details of proteins in the specific crystal packing; however, cryo-EM map is reconstructed from thousands of particles in different views. As the substrate is moving constantly in the channel, AQP7 cryo-EM structure may provide additional valuable information for the dynamic of glycerol. Thus, to illuminate the discrepancy of substrate in-between channels, HOLE analysis was performed for all eight chains (A-H) in cryo-EM structure as well as crystal structure, respectively. Clearly, glycerol density presents in all individual channels but in a varying degree, however, the density in proximity of NPA motif was well-defined in all eight channels, suggesting that glycerol interacts with NPA motif tightly (Fig. 21A). Additionally, rather different channel dimensions were discovered among different chains in cryo-EM structure, and all individual channels presented narrower ar/R filter than that of crystal structure (Fig. 21A). Accordingly,

aromatic rings of F74 and Y223 in chain A move 0.4 Å and 0.6 Å, respectively, as compared with those in crystal structure, thereby resulting in radius difference of approximate 0.22 Å at the position of ar/R filter between chain A and crystal structure (Figs. 21A-B).

To further study the potential association between loop C and dimer formation of AQP7, the loop C of AQP7 crystal structure was aligned to the cryo-EM structure. In contrast to AQP7 crystal structure, P151 and V152 in cryo-EM structure show 3.7 Å and 1.4 Å shift, respectively (Fig. 21C). Additionally, the central pore of AQP7 in cryo-EM structure formed by four monomers is wider than that of crystal structure, leading to the minor shift of tetramerization between structures (Fig. 21D). The central pore in crystal structure is typically affected by crystal packing and four-fold symmetry, however, cryo-EM harbours advantages of that the protein is frozen rapidly in "near-native" state and not affected by crystal packing[97], thus providing the possibility for the study of central pore.

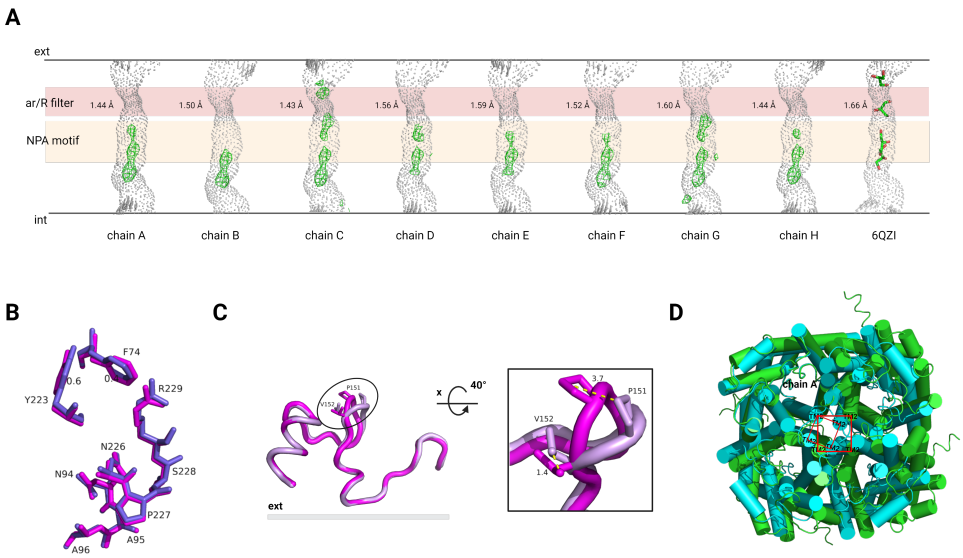

Figure 21. The structural alignment between AQP7 crystal structure (PDB ID:6QZI) and cryo-EM structure. (A) HOLE analysis for all individual channels in cryo-EM structure and crystal structure. (B) The alignment between chain A (blue) in cryo-EM structure and crystal structure (magenta). The residues at position of ar/R and NPA motif are shown as sticks, and the movement of F74 and Y223 between two structures are measured and shown. (C) The extracellular loop C in AQP7 crystal structure aligned with AQP7 cryo-EM structure. P151 and V152 represented by sticks show significant shift between two structures, and the distances were labeled by yellow dash line by measuring the shift of atom CG in P151 and CG1 in V152, respectively. (D) The tetrameric packing formed by AQP7 monomers (cyan, PDB ID:6QZI) was aligned with tetramer in AQP7 cryo-EM structure (green). TM2 in both structures relevant with the formation of central pore were marked and connected by heavy and light red line, respectively, to highlight the shift of tetramerization (Adapted from figures in Paper IV).

AQPs central pore and relevant substrate diffusion

It is well known that each monomer of AQPs can function as an independent water or glycerol channel, however AQPs usually adopt the tetrameric configuration, thus facilitating the formation of central pore by four monomers. The potential function of the central pore is still debated. Firstly, human AQP1 was reported to have the capability of cation conduction through central pore activated by binding with cGMP and a series of conformational changes of loop D[98-101]. Also, it was proposed that the central pore of AQP1 is a possible pathway for small, neutral gas molecules, such as CO2 and O2[102]. Additionally, a lipid was observed in the central pore of human AQP5, and thus occluding the pore and preventing the passage of other molecules, such as ions or gases[100]. Interestingly, similar scenario was also found in AQPZ[101]. Herein, AQP7 structure was resolved by cryo-EM, not affected by crystal packing and pseudo central axis, and thus relevant for detailed structural analyses of central pore. Interestingly, well defined densities are observed in the central pore of each AQP7 tetramer, confined by four leucines at the intra- and extracellular sides, named as leucine filters (Fig. 22A). Both densities display the dimension accommodating one or two glycerols and two water molecules (Fig. 22A) but are too small to accommodate the lipid that was fitted in the central pore of AQP5[103]. Although the central pore of AQP7 is lined by hydrophobic residues, in a similar manner as in AQP5[103], the cavity restricted by leucine filters is positively charged (Fig. 22B). Thus, small intermediate metabolites involved in glucose, lipid, and cholesterol metabolism in human adipocytes, such as glycerol-3-phosphate (Gro3P) and isopentenyl pyrophosphate (IPP)[104] and their derivatives, DHAP, G3P and dimethylallyl pyrophosphate (DMAPP) are considered as possible ligands (Fig. 22C), all showing good fitting with the densities (Fig. 22D). Hence, it is reasonable to speculate that AQP7 dimer of tetramers facilitates intercellular diffusion of small metabolic products through the central pore by forming gap junctions between cells in human adipose tissue. However, this needs to be further confirmed by experimental data.

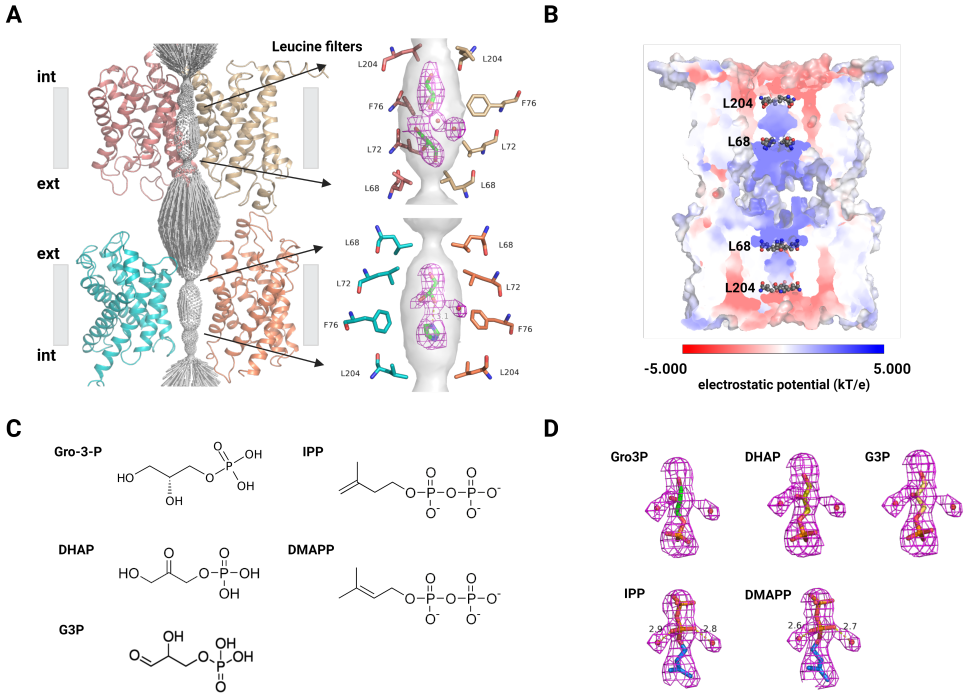

Figure 22. The central pore of human AQP7 cryo-EM structure. (A) HOLE analysis and leucine filters of central pore. Hole of central pore and pore lining residues are shown as dots and sticks, respectively, while cryo-EM density in central pore is represented by magenta mesh. Glycerol, imidazole and water molecules, components in the sample buffer, are fitted into densities. (C) Chemical structures of potential ligands in central pore. (D) The density in central pore of lower half tetramer fitted with possible ligands. The distance between oxygen atom of water and IPP/DMAPP is measured (Paper IV).

Gap junction relevant AQPs

AQP0 is a water channel abundantly expressed in lens fibre cells, and particularly located in the thin junctions featuring orthogonal arrays[105]. AQP0 has been shown to form double-layered 2D crystals and suggested to be physiologically relevant with thin junctions between fibre cells, thus AQP0 may serve as an adhesion molecule between cells apart from functioning as a water channel[106]. Analogously, AQP4, a major water channel in brain, has also been shown to form orthogonal arrays in vivo as well as in 2D crystals, implying that AQP4 also functions physiologically as cell adhesion molecule[107]. Two AQP0 tetramers associate with each other in the crystal packing via loop A and loop C in the straight manner, and the rearrangement of loop A mediated by termini proteolytic cleavage is crucial for AQP0 junction formation[106,108] (Fig. 23A). AQP4 tetramer instead interacts with four tetramers in the opposite layer in the crystal packing by the extracellular C loops (Fig. 23B). In contrast to both AQP0 and AQP4, AQP7 adopts the formation of octamer in a twisted stacked manner with two tetramers interacting with each other by the protruding loop C through residues P151 and V152 from all eight monomers (Figs. 23C and 20B). The whole octamer of AQP7 displays a height of 10 nm in which extracellular region between two tetramers is around 3.3 nm, compared to 2.5nm and 2.2nm for AQP0 and AQP4, respectively (Figs. 23A-B and 19A). Thereby, it is proposed reasonably that AQP7 dimer of tetramers, in analogy to AQP0 and AQP4 may serve as a gap junction and/or adhesion molecule between adjacent cell membranes.

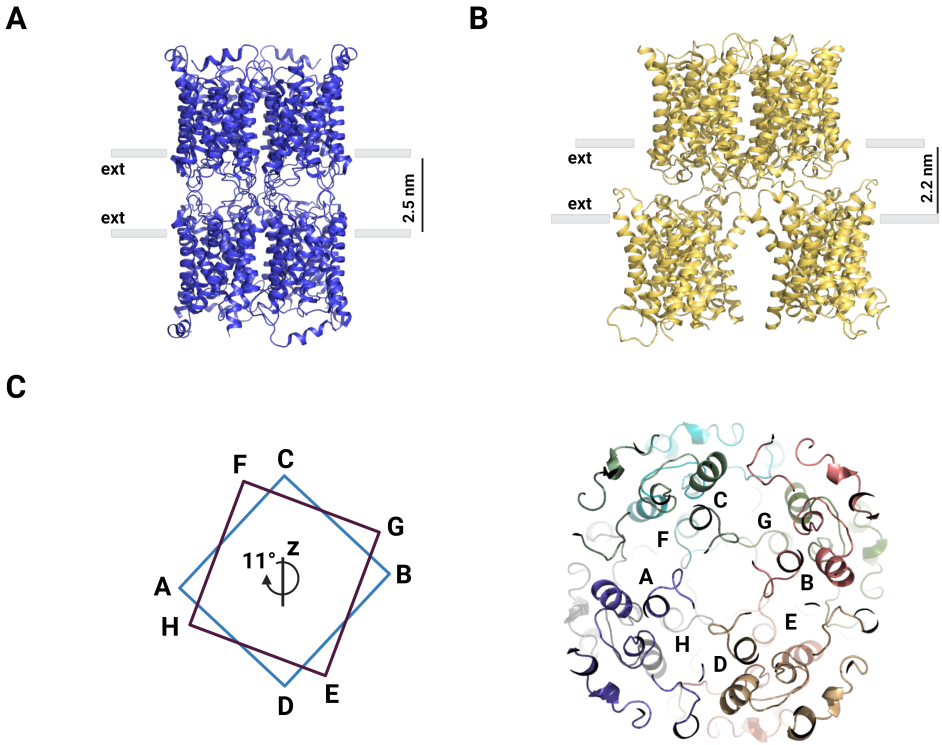

Figure 23. Gap junction forming AQPs. The crystal packing form of (A) AQP0 (PDB ID: 2B6O) and (B) AQP4 (PDB ID: 2D57). (C) The arrangement of two tetramers in a twisted manner with a rotation of approximate 11° around z axis. The left figure is a simplified diagram illustrating the twisted form of two tetramer, in which letters A-H represent eight subunits in octamer. All figures are referred from paper IV.

Summary

The adipose tissue primarily comprising of adipocytes (storage of energy as TAG) is a central metabolic organ for carbohydrates and lipids to maintain the overall energy homeostasis in the human body. Glucose transported into the cells from blood circulation via GLUTs upon insulin stimulation, is the starting substrate for glycolysis and subsequent lipogenesis. Gro3P synthesized from glycolysis is on the crossroad connecting glucose and lipid metabolism and serves as a necessary substrate for lipogenesis. The TAG is hydrolysed into fatty acid and glycerol efflux from adipocytes via AQPs when the hydrolysis is induced upon adrenergic stimulation after fasting or exercising. Thereby, glucose transport and glycerol efflux play a detrimental role in maintaining metabolic balance in human adipocytes, and their dysfunctions are tightly associated with type II diabetes, obesity, and hyperglycaemia.

Human primary adipocytes are unilocular cells with a single lipid droplet taking up most of cell space and squeezing the nucleus to the periphery of cell and the cytoplasm becomes a thin rim. Thus, confocal microscopy is not optimal to study adipocytes ultrastructure and detailed subcellular localization of proteins. Instead, TEM combined with immunogold labelling technique displays better visualization for cell structure and protein localization in adipocytes (**Paper I**).

GLUTs are a family of membrane proteins facilitating hexose transport down concentration gradient. The transcriptome sequencing analysis presents that GLUT1, GLUT3, GLUT4 and GLUT5 are expressed significantly at mRNA level in adipocytes. Unlike other GLUTs, GLUT4 is expressed exclusively in adipocytes and muscles cells. Moreover, it is well known that GLUT4 translocate from cytoplasmic compartments to plasma membrane upon insulin signal, a process known as GLUT4 trafficking. In rodents, TUG serves as a tether by forming complex with GLUT4. Upon insulin stimulation, TUG is cleaved endoproteolytically and thus releasing GLUT4 and facilitating the trafficking of GLUT4 to cell membrane to mediate glucose uptake. ASPL is the homologue of TUG in human, and in the study, ASPL is shown to interact with GLUT4 by binding to its intracellular helical bundle via C-terminal UBX domain and potentially regulate GLUT4 trafficking in the similar manner as in rodents (**Paper I**).

AQPs are membrane channels mainly mediating the flux of water and glycerol through cell plasma membrane. Aquaglyceroporin 7 (AQP7) is a glycerol channel

abundantly expressed in adipose tissue and it facilitates glycerol efflux from the cytoplasm. PLIN1 is the binding partner of AQP7 on the surface of lipid droplet and a regulator for lipolysis by releasing AQP7 upon catecholamine activated phosphorylation. In **paper II**, we found by transcriptome sequencing and RT-PCR that *AQP1*, *AQP3*, *AQP7* and *AQP9* genes are expressed in the human primary adipose tissue, and that *AQP7* shows significantly higher expression level. Furthermore, we show by BN-PAGE that the C-terminus of PLIN1 is binding with AQP7. Additionally, we also discovered that AQP3 binds with PLIN1 in addition to AQP7, implying that AQP3 and AQP7 partly have redundant role in human adipocytes during lipolysis.

To understand the detailed function of GLUT4 we aimed to determine the structure of GLUT4, and thus rat GLUT4 was expressed heterologously in *Pichia pastoris*, and the detergents screening indicated that DM is the optimal detergent for GLUT4 solubilization from yeast membrane. GLUT4 was purified by affinity chromatography followed with SEC, and purified protein presented single particle distribution in negative staining. Moreover, putative docking models were generated by imposing distance constraints below 33 Å for each pair of crosslinking sites, suggesting GLUT4 forms complex with ASPL by utilizing its ICH domain to bind with both UBL2 and UBX domains in ASPL (**Paper I**).

Cancer cells show high energy demand and increased glucose metabolism compared to normal cells, known as Warburg effect. Thus, GLUTs are potential drug targets for treatment of cancers. In **paper III**, we studied the inhibiting mechanism of PGL13 and PGL14 on GLUT1 from the structural level by applying of MD simulation in combination with intrinsic tryptophan quenching. The data suggested that PGL13 and PGL14, as novel GLUT1 inhibitors, likely block glucose uptake by binding both sites of transmembrane and intracellular domains, and thus sensitizing acute myeloid leukemia (AML) to chemotherapy.

In **paper IV**, AQP7 structure was determined at 2.55 Å resolution by cryo-EM adopting a dimer of tetramers. The two tetramers dimerize by hydrophobic interactions imposed by P151 and V152 located at protruding extracellular loop C with a rotation of approximate 11° along the central axis between the tetramers. As the AQP7 cryo-EM structure is not affected by crystal packing, the central pore in cryo-EM structure was investigated and shown to be wider than that of crystal structure. The central pore formed by four monomers is restricted by two leucine filters located at the intra- and extracellular sides, respectively. Interestingly, well-defined densities are identified in the two central pores, compatible with small metabolites in glucose, lipid, and cholesterol metabolism, such as Gro3P, DHAP, G3P, IPP and DMAPP. Thus, we speculate that the identified AQP7 dimer of tetramers may serve as gap junctions to facilitate metabolite diffusion through the central pore between cells in human adipose tissue, although this still require further experimental validation.

Concluding remarks and future perspectives

In this study, we are dedicated to investigating glucose and glycerol transport in human adipocytes from structural perspectives, specifically on the study of mRNA expression level of GLUTs and AQPs, protein interactions between GLUT4 and ASPL (PLIN1 and AQP7/3), GLUT4 expression and purification towards the structural study, docking model of ICH_{GLUT4} and ASPL-C, GLUT1 inhibitor and structural determination of AQP7 by single particle cryo-EM.

Multiple approaches were applied in our study (Paper I) and suggested that GLUT4 binds ASPL-C by its ICH domain, and potential docking models were generated for the interacted domains between GLUT4 and ASPL, showing both UBL2 and UBX domains in ASPL may involve in the interaction with GLUT4. To confirm this further, site-directed mutagenesis for the crucial residues followed by binding assay to evaluate the rationality of docking model can be performed. Interestingly, both GLUT4 and ASPL were suggested to be localized in cytoplasm of adipocytes in the basal state. To investigate whether they interact *ex vivo* in adipocytes and how ASPL regulates GLUT4 trafficking upon insulin stimulation, further investigations are needed.

Elucidating the structure of GLUT4 is important to understand the mechanism of GLUT4 trafficking and glucose uptake in adipocytes. Rat GLUT4 was expressed in yeast successfully and initial detergent screening was performed for membrane solubilization. Purified protein showed single particle distribution in negative staining, even though it was not homogeneous in the SEC, which suggests that cryo-EM might be a promising approach to resolve GLUT4 structure. GLUT4 is a protein in the molecular weight of 54 kDa approximately, which is still a bottleneck size for the structural determination by cryo-EM, particularly, other GLUTs show featureless structure on both intra- and extracellular sides. However, this could be circumvented by preparing GLUT4 in complex with ASPL, leading to increased particle size and likely improved distribution and orientation of particles on the grid.

The genes of *AQP7*, *AQP3* and *AQP9* showed significant expression in human adipocytes. It was reported previously that the glycerol hinders rapid water flux through AQP7[36], suggesting a specific water channel may exist on the membrane of adipocytes to maintain osmotic homeostasis. This agrees with our transcriptome

sequencing and RT-PCR data where *AQP1* was expressed at significant level. AQP7 is most abundantly expressed glycerol channel in adipocytes, and AQP7 was suggested to bind to PLIN1 on the surface of lipid droplet in basal state. Here we found that hydrophilic C-terminus of PLIN1 (PLIN1-C) is important for the binding to AQP7. Moreover, PLIN1 regulates lipolysis by controlling the access of HSL and ATGL to the lipid droplet[3,5,73], however, structural information of PLIN1 has not been revealed yet, likely due to its hydrophobic nature. Thus, deciphering the complex structure of AQP7 and PLIN1 (or PLIN1-C) would provide insights on the regulation mechanism of AQP7 translocation and lipolysis.

In addition to AQP7, AQP3 was also suggested to form complex with PLIN1-C. AQP3 is indicated as a glycerol channel and probably also facilitates glycerol efflux from adipocyte[51], however, the function of AQP3 in details in adipocytes remains unclear. Hence, it would be valuable to elucidate AQP3 glycerol conducting mechanism at structural level.

AQP7 structure was determined at the resolution of 2.55 Å by single particle cryo-EM, showing that AQP7 can form a dimer of tetramers with the height of approximate 10 nm. It has previously been suggested that AQP7 is expressed in the capillary endothelial cells in white adipose tissue[38], in addition to adipocytes. Thereby, it's reasonable to speculate that AQP7 may serve as gap junction or adhesion molecule by forming dimer of tetramers between adjoining two adipocytes or one adipocyte and the neighbouring endothelial cell. This can be identified by immunogold labelling of AQP7 in adipose tissue in future work. Moreover, well-defined densities were discovered in the central pore, showing good fitting with small intermediate metabolites involved in glucose and lipid metabolism. This suggests that AQP7 may facilitate the diffusion of small metabolites through central pore between adjacent two cells. Gro3P is a potential molecule diffusing in-between cells through central pore of AQP7, as no specific Gro3P has been identified in humans[109]. Gas chromatography mass spectrometry (GC-MS) is being performed to reveal the identity of the ligands in central pore. In addition, transporting assays and MD simulation can also be applied to elucidate the diffusion mechanism of the ligand through central pore.

Providing that AQPs are involved in many important physiological and pathophysiological processes and its expression levels correlate with tumors development[110], they are potential therapeutic targets for cancer therapy. Mouse models of AQP3 knockout or knockdown showed suppression of skin tumorigenesis and tumour growth in non-small cell lung cancer and migration of breast cancer cells[111-113]. Additionally, AQP7 was also suggested to be a crucial regulator for the metabolism and signal response of breast cancer cells[114]. Furthermore, glycerol metabolism mediated primarily by AQP7 as well as AQP3 is associated tightly with the metabolism of lipid and carbohydrates, thus playing an important role on the regulation of glucose homeostasis, insulin sensitivity and fat accumulation in adipocytes[115]. Thereby, the study of inhibitors of AQP3 and AQP7 from structural

perspective could provide evidence and support for the development of AQP3 and AQP7 as therapeutic targets in cancers and metabolic diseases. In contrast to X-ray crystallography, single particle cryo-EM presents advantages of crystal-free; quick process of sample preparation, maintaining sample in “native” and even multiple conformational states, and high reproducibility. Thus, cryo-EM may be become a promising technique employed in the structural study of inhibitors in complex with AQP3/AQP7.

Methodology

My work in the thesis mainly focuses on the studies of PPI by the combination of biochemical and biophysical approaches, subcellular localization of proteins of interest applying microscopical techniques and structural determination of membrane protein (AQP7) using cryo-EM. However, the production of good-quality recombinant proteins is the prerequisite for the study of PPI *in vitro* and structural determination of proteins. Herein, different expression systems for recombinant proteins are introduced, and methods applied in the study of PPI are compared, electron microscopical techniques utilized in the work, including immunogold labelling, negative staining TEM and single particle cryo-EM are described briefly.

Expression systems of recombinant proteins

The production of recombinant proteins is starting point for most biochemical and biophysical analyses of proteins. The expression systems commonly used include prokaryotic and eukaryotic hosts, such as bacteria, yeast, insect cells and mammalian cells. All these systems have advantages and disadvantages; thus, the best choice might be the one that fits the target protein best.

The bacterial expression host, usually *E.coli*, is widely used for heterologous production of proteins. It has advantages of simple operation, low cost, high yield and well-characterized biochemistry and genetics[116]. Thereby, in this work, almost all soluble proteins, e.g., ASPL, ASPL-C, Trx (Thioredoxin), Trx-ICHGLUT4, PLIN1-C were expressed in *E.coli*, and showed satisfactory quality and yield for downstream purification. However, the proteins expressed in this host lack some post-transcriptional modification (PTM) observed in eukaryotes, and thus human proteins are prone to aggregate. The solubility of the expressed protein may be improved by the addition of fusion tag or the co-expression with molecular chaperones[117]. Herein, both ASPL and ASPL-C were tagged with GST (glutathione-S-transferase) while ICH_{GLUT4} were fused with Trx, and as a result they showed good solubility in the expression.

Yeast is a common eukaryotic host for protein expression. Yeast is growing rapidly and adaptable to the process of fermentation, enabling to achieve high cell density

and protein yield. In contrast to *E.coli*, yeast can modify the protein with PTM, although N- and O-linked glycosylation patterns produced in yeast may be different with those in higher eukaryotes. *P. pastoris* and *S. cerevisiae* are two yeast expression hosts commonly used for protein production, specifically for structural study of integral membrane proteins[118]. However, compared with *S. cerevisiae*, *P. pastoris* showed higher yield of protein and less glycosylations for glycoproteins[119,120]. Moreover recombinant proteins expressed in *S. cerevisiae* may undergo proteolytic cleavage associated ubiquitin-proteosome system[121]. On the other hand, *S. cerevisiae* presents the advantages of using cytoplasmic expression vector in no need of fusion with genome and convenient selection for positive transformants as compared to *P. pastoris*[122]. In our study, human AQP7 and rat GLUT4 were expressed in *P. pastoris* and further purified before structural studies. Of note is that 3D-structures of membrane proteins in families of GLUTs and AQPs including human AQP2[90], human AQP5[92], human AQP10[57], human GLUT1[123] and rat/bovine GLUT5[78] were determined by using protein samples expressed in yeast.

In contrast to *E.coli* and yeast expression systems, baculovirus-infected insect cells and mammalian cells are capable to perform PTMs of target proteins, similar to higher eukaryotes[124]. The insect cell expression system has been the prevailing system for heterologous production of eukaryotic membrane proteins and can facilitate correct folding of proteins and formation of tertiary and quaternary structure[120,125]. An advantage of mammalian expression host which insect cells lacks is that they can be utilized to produce complex glycoproteins and recombinant proteins for human therapy[120]. However, both insect cells and mammalian expression system show drawbacks likely limiting their wide use in practice, such as slow cell growth, limitation of culture equipment, high costs and time-consuming and laborious production, and sometimes low protein yields[120].

Protein and protein interaction (PPI)

Here, antibody-based biochemical and biophysical methods utilized for the study of PPI (GLUT4 and ASPL, AQP7 and PLIN1) in my work are introduced and compared. Although most of approaches show advantages and disadvantages, they can be applied in a combined and complementary manner, providing insight on the choice of methods in the future PPI study.

Antibody-based biochemical methods

In the study, pull-down assay, far dot western blot and BN (blue native) -PAGE were applied to investigate the protein interaction between GLUT4 and ASPL/AQPs and PLIN1. Pull-down assay is a conventional and widely used

approach in the study of proteins interactions in which the interaction is identified by antigen-antibody reaction. Similarly, far dot western blot detects proteins interaction by antibodies against the protein of interest and shows the benefit of maintaining proteins in their native three-dimensional structure. Specifically, the technique allows multiple bait proteins to be immobilized on nitrocellulose membrane upon the incubation of a prey protein, thereby being commonly used for rapid screening of potential protein and protein interactions[126]. Both pull-down assay and far dot western blot have the capability to detect the interaction between the protein of interest with possible binding partner in cells by applying the cell lysate. In our study, the interaction between purified ASPL and GLUT4 expressed in yeast was identified by pull down (Paper I) while the binding of pure PLIN1-C and AQP7/3 solubilized in yeast lysate was detected via far dot western blot (Paper II). By contrast, BN-PAGE amenable to antibody examination is preferred to be utilized in the analysis of the complex formation by monitoring the mass shift on the gel without breaking their native conformation. Also, it can provide information for possible stoichiometry within protein complex by applying different ratios of interest of proteins onto the gel[127]. Herein, the complex formation of AQP7 and PLIN1-C was confirmed by BN-PAGE, and it was suggested that one AQP7 may bind more than one molecule of PLIN1-C (Paper II).

Biophysical methods

One drawback with biochemical approaches based on antigen-antibody reactions for PPI is that it may fail to detect weak and transient proteins interactions. Another drawback is that it is prone to produce unspecific binding, thus leading to false positives. Thereby, biophysical techniques, such as isothermal titration calorimetry (ITC), nuclear magnetic resonance (NMR), surface plasmon resonance (SPR) microscale thermophoresis (MST) and mass spectrometry (MS) etc., are being employed instead, or serving as complementary tools to biochemical methods. Most of them are optical approaches recording certain physical phenomenon and converting them into data signal from which the affinity of interaction can be calculated, and thus showing good sensitivity for weak interactions and data reproducibility[128]. Herein, we applied SPR and crosslinking mass spectrometry (XL-MS) to confirm the interaction between ICH_{GLUT4} and ASPL-C and identified crucial residues locating at the interface of proteins interaction. In contrast to other biophysical approaches, SPR is label-free and real-time monitoring, and needs low amount of sample for the determination of both association and disassociation rate constants, while XL-MS allows to identify the proximal structural fragments between interacting proteins, and crosslinked residues pairs identified by MS provide geometric restriction for molecular docking[129].

Electron microscopical techniques used in the study

TEM has been widely applied for the high-resolution visualization of tissue/cell and biological macromolecules. Here, we apply TEM combined immunogold labelling to visualize human adipose tissue and carry out the study of subcellular localization of GLUT4 and ASPL in adipocytes. In addition, negative staining TEM was utilized to perform pre-analysis of AQP7 particles before cryo-EM. Single particle cryo-EM was compared with X-ray crystallography and introduced from workflow to sample preparation by taking AQP7 as an example.

Immunogold labelling

Immunogold labelling is a negative staining technique of biological tissues and cells combined with TEM, including two modes, pre-embedding, and post-embedding. Herein, we utilized the approach of post-embedding immunogold labelling to identify proteins of interest in human adipose tissue by performing immunocytochemical procedures after tissue embedding, as post-embedding mode is more likely to keep the structural intactness of tissues and cells[130]. In principle, colloidal gold particles are conjugated with secondary antibodies to be bound onto primary antibodies against interest of molecules, and thus the position of gold particles represent the potential subcellular localization of proteins. The size of gold particles is optional ranging from 5 nm to 40 nm depending on the experimental requirements, and thus multiple antigens can be labelled by utilizing gold particles with different size. Moreover, gold particles are eligible to scatter more electrons, thereby producing strong contrast. Although colloidal gold particles are commonly used as markers in the technique of immunogold labelling, there are some other types of electron-dense antibody conjugates available, such as uranium[131], ferritin[132], and iron-dextran etc[133]. However, a drawback is that the location of the gold particles may not represent the accurate subcellular localization of proteins, as the gold particle is 15-30 nm away from the antigen, determined by the length of antibody[134]. Importantly, if the precise localization of the proteins of interest are studied, quantitative analysis is necessary[130].

Negative staining TEM

Negative staining is a widely utilized technique to prepare biological specimens to image by TEM (Fig. 24A). Herein, we applied this technique to visualize purified membrane proteins (GLUT4 and AQP7) (Figs. 15E and 24B), providing information important for further single particle cryo-EM grid preparation. Shortly, biological specimens are embedded in the stain of heavy metal salt, e.g., uranium (U), vanadium (V), tungsten (W), gold (Au), lead (Pb) and osmium (Os), etc., scattering electrons more strongly than those elements comprising biological

molecules (i.e., C, H, O, N, P, S) to increase the contrast between the stain and the samples[135] (Fig. 24A). Negative staining is an effective tool for rapid assessment on morphology, distribution, and homogeneity of protein of interest before applying cryo-EM or optimization of cryo-grid conditions[136]. Moreover, with the development of computational software, the images of negatively stained samples can be classified and reconstituted, however, due to preferred orientation of protein particles and crystals formed by heavy metals in the solution of negative staining, the resolution of reconstituted map is limited to approximately 20 Å[137], so far. In our study, AQP7 was negatively stained by uranyl acetate and visualized via TEM presenting homogeneous and even single particles of approximately 10 nm on the grid, laying the foundation for further cryo-EM study for AQP7 (Fig. 24B).

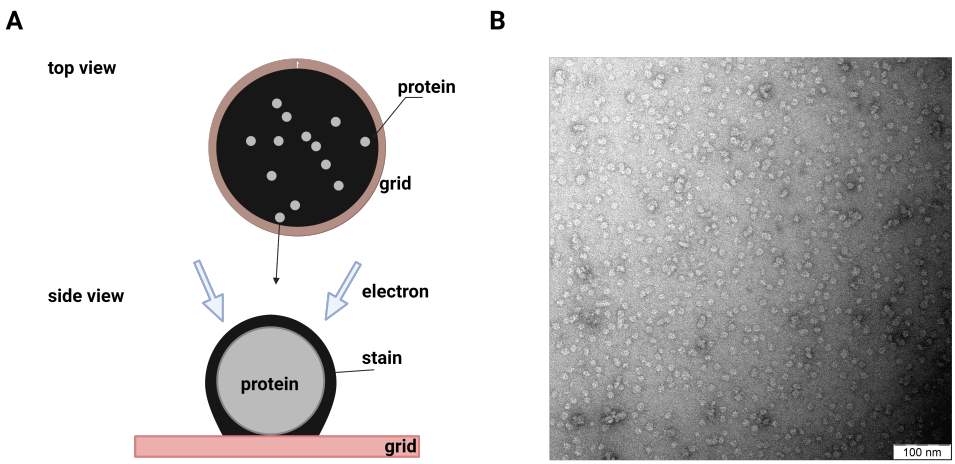

Figure 24. Negative staining TEM. (A) Schematic representation of negative staining. (B) Negative staining image of AQP7 solubilized in digitonin.

Single particle cryo-EM

During recent years, single particle cryo-EM has revolutionized three-dimensional (3D) structural determination of biological macromolecules. This is attributed to the breakthroughs of hardware and software of cryo-EM, in combination with improved molecular biological techniques resulting in models at the near-atomic resolution to be determined from reconstituted 3D map[138].

Herein, we determined the structure of human AQP7 by single particle cryo-EM. The starting point of cryo-EM workflow (Fig. 25) is the preparation and optimization of protein samples suitable for cryo-EM. Cryo-EM samples of AQP7 was prepared and optimized either in the detergent digitonin/glyco-diosgenin

(GDN), or by reconstituting AQP7 into amphipol/nanodisc before the sample was further polished by size exclusion chromatography (SEC). Negative staining TEM was used for the initial evaluation of sample quality and particles distribution on the grid, but this step is optional. The optimized protein sample was applied onto grid coated with a thin film (e.g., carbon and graphene), and vitrified by submerging the grid into a cryogen (liquid ethane is usually used) by which the sample was suspended in a thin layer of vitreous ice, the process known as plunge freezing[139]. Here, the optimization on the grid type, freezing condition, sample amount and concentration and buffer composition, and blotting force and time, etc., is necessary to obtain a good enough grid with even particles distribution and appropriate ice thickness and contrast for data collection. Images were collected by 300 kV cryo-electron microscopy (Titan Krios), followed by computational processing via cryoSPARC[140], although some other programs used for data process of cryo-EM are available[141]. In the data process, the images were corrected upon beam-induced motion and contrast transfer function (CTF)[140] before target particles were selected and extracted. Subsequently, these particles were aligned, and particles with similar features were classified, termed as 2D classification. Typically, 2D classification can be run for multiple cycles to exclude more "junk" particles. Subsequently, particles with well-resolved features were reconstructed into initial 3D map which will be further refined until high resolution map was generated. Finally, the model was built from cryo-EM map and refined to get accurate structural information.

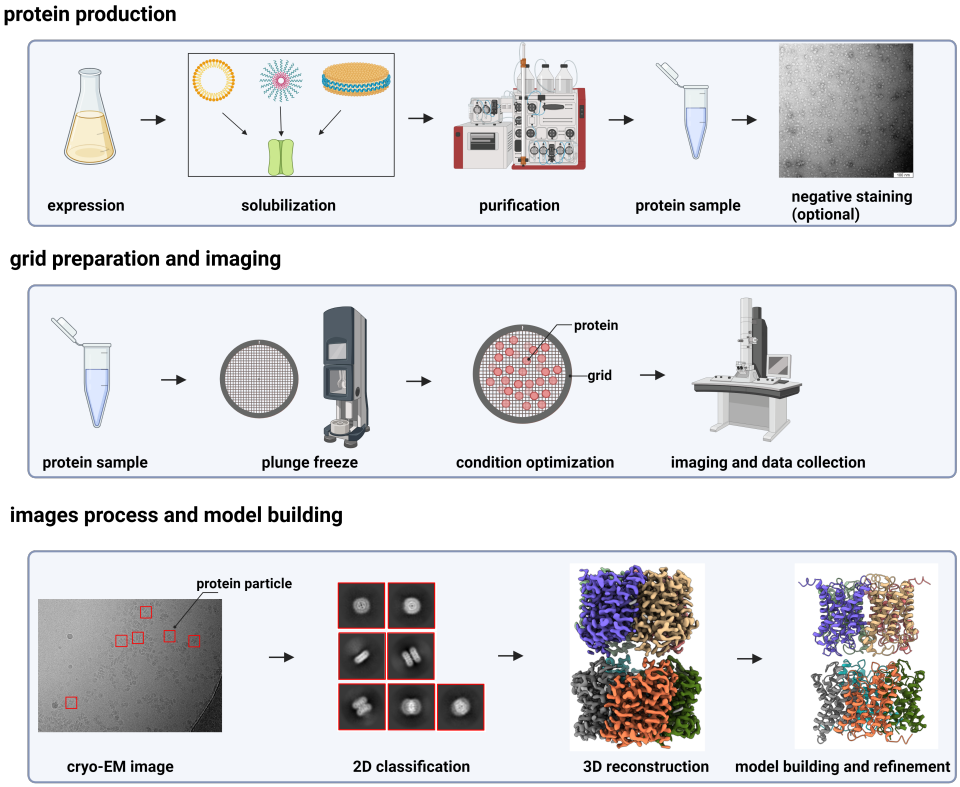

Figure 25. Workflow of single particle cryo-EM.

X-ray crystallography in comparison with single particle cryo-EM

Although cryo-EM is booming, X-ray crystallography still represents one of mainstream techniques in the structural biology and is capable to resolve protein structures at atomic resolution. X-ray crystallography is applied for the structural determination of soluble proteins, membrane proteins as well as protein complexes, and is not limited by molecular mass of targets to be crystallized, which is, in contrast to cryo-EM that has higher size-limit (Table 3). Moreover, a significant advantage of X-ray crystallography is that it is prone to generate high-resolution and precise structural information, as the crystals are packed orderly in the lattices, thus restricting their motions[142]. However, a prerequisite for crystallography is to get a well-ordered crystal before the diffraction can be collected, which is not needed in cryo-EM. Although many types of protein can be crystallized, getting a well-diffracted crystal needs thorough optimization, such as protein concentration, homogeneity, post-translational modification, and buffer composition, temperature etc. Unlike crystallography, the molecules in cryo-EM are not constrained by crystal packing, hence the conformations captured by cryo-EM is more likely to be in their

"near-native" states[97]. On the other hand, the flexibility of molecules and heterogeneity of samples might compromise the final resolution of 3D map computed by cryo-EM, still it may generate a benefit since more conformations of the proteins could be recorded. This provides the possibility to elucidate the working mechanism of proteins functioning through conformational switches by less effort than crystallography. Typically, X-ray crystallography and cryo-EM can be complementary to decipher structural information of biological molecules depending on the demand of users[97,143].

Table 3. The comparation of X-ray crystallography and single particle cryo-EM.

X-ray crystallography	Single particle cryo-EM
• No size requirement for samples	• No strict limitation for sample size, good for biological macromolecules and protein complexes, but additional strategies are required when molecular weight is smaller than 50 kDa[144]
• Sample consuming	• Significantly lower sample consumption
• Well-ordered and -diffracted crystal is required	• Sample in solution
• Crystal packing may distort protein structure	• The sample is plunge frozen in "near-native" state
• Flexible and nonhomogeneous samples are hard to get well-diffracted crystals	• No strict requirements for sample flexibility and homogeneity
• Reach atomic resolution	• Reach near-atomic resolution
• Resolve precise atomic coordinates, and resolution ultimately depends on the degree of order in crystal packing	• The resolution is calculated in different way from X-ray crystallography[97]
• Static conformation is captured from crystal diffraction	• Multiple conformational states can be resolved from heterogeneous data

Cryo-EM sample preparation of membrane protein: detergent, polymer and nanodisc

Traditionally, membrane proteins are extracted from membranes and solubilized in detergents above their critical micelle concentration (CMC). Detergents are amphipathic molecules that solubilize membrane proteins in water solution by forming micelles embedding transmembrane domains of the proteins (Fig. 26A). However, an excess of detergents in cryo-EM samples may negatively affect the surface tension of grids, ice thickness and background of images[145]. Thereby, detergents with small CMC are preferred to be applied in the study of cryo-EM, such as dodecyl-β-D-maltopyranoside (DDM) and maltose-neopentyl glycols (MNGs), digitonin and its substitute GDN, etc. Another disadvantage utilizing detergents in sample preparation of membrane proteins, is that they could displace native-binding lipid from the protein and interfere hydrophobic interaction in-between helices, thus destabilizing the membrane protein[146]. Similar as detergents,

amphipols are a series of amphipathic polymers and stabilize membrane proteins in aqueous solution by forming well-defined and small globular particles around hydrophobic domains (Fig. 26B). In contrast to detergents, amphipols has higher affinity for transmembrane domains even in low concentration and hence free amphipols rarely exist in the solution[147,148]. Additionally, amphipols show the capability of stabilizing membrane proteins better than detergent micelles[149,150], and assisting membrane protein folding to their native form[151]. The amphipol A8-35 is one of most used amphipols for cryo-EM. Another alternative is nanodiscs which constitute of lipids and two encircling amphipathic membrane scaffold proteins (MSP), thus stabilizing membrane proteins in a detergent-free membrane resembling environment (Fig. 26C). In addition, the nanodisc has been suggested to stabilize conformations of membrane proteins which are less well resolved in detergent and amphipol samples[145]. However, in practical, obtaining a type of MSP with appropriate diameter and an optimal lipid-MSP-protein ratio may be challenging, but necessary for sample stability and high-resolution structural determination. In contrast to lipid nanodiscs, amphipol can be used to substitute detergent for the protein extraction from membrane[148], however, solubilizing membrane protein in detergent is still a prerequisite for nanodisc sample preparation.

During the long-term endeavour to resolving the cryo-EM structure of AQP7, we have tried to solubilize and stabilize AQP7 in GDN, amphipol A8-35 and nanodiscs, to retrieve stable, homogeneous protein sample, and prepare grids with well-distributed particles and acceptable ice thickness and signal-noise-ratio. AQP7 was stable and homogeneous in each of them (Fig. 26), but it showed different oligomeric states in GDN, amphipol A8-35 and nanodisc. Specifically, AQP7 did not form dimer of tetramers in amphipol and nanodisc (Fig. 26B-C). In addition, protein particles stabilized by amphipol and nanodisc showed preferred orientation resulting in missing views (Fig. 26B-C), which imposed negative effect on 3D reconstruction. Finally, AQP7 structure adopting the formation of dimer of tetramer was resolved in GDN detergent (Figs. 26A and 19). As described above, amphipol and nanodisc may improve the stability of membrane proteins, but such that the flexibility of proteins can be constrained, thus likely causing the issue of preferred orientation and the absence of important conformational states in our case.

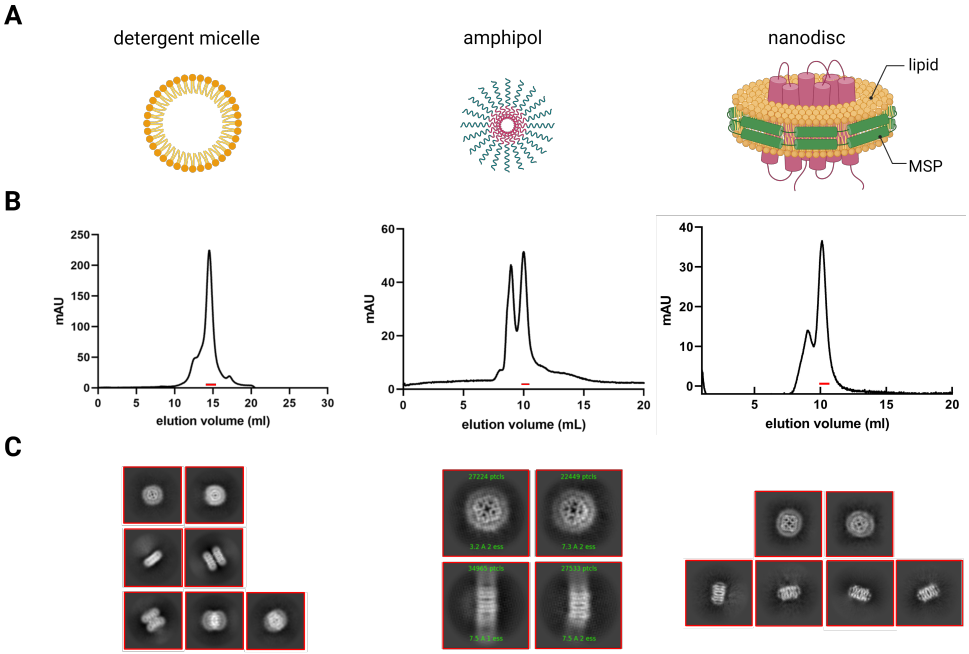

Figure 26. AQP7 cryo-EM sample preparation in GDN, amphipol A8-35 and nanodisc. (A) Schematic representation for detergent micelle, amphipol and nanodisc embedding membrane protein colored in magenta. (B) SEC profiles of AQP7 purification in GDN, amphipol A8-35 and nanodisc (from left to right). The red line represents the fraction used for grid preparation and data collection. (C) 2D classification images for protein particles stabilized by GDN, amphipol A8-35 and nanodisc (from left to right).

References

1 Yu, C., Cresswell, J., Löffler, M. G. & Bogan, J. S. The glucose transporter 4-regulating protein TUG is essential for highly insulin-responsive glucose uptake in 3T3-L1 adipocytes. J Biol Chem 282, 7710-7722, doi:10.1074/jbc.M610824200 (2007).

2 Li, D. T. et al. GLUT4 Storage Vesicles: Specialized Organelles for Regulated Trafficking. Yale J Biol Med 92, 453-470 (2019).

3 Miyoshi, H. et al. Perilipin promotes hormone-sensitive lipase-mediated adipocyte lipolysis via phosphorylation-dependent and -independent mechanisms. J Biol Chem 281, 15837-15844, doi:10.1074/jbc.M601097200 (2006).

4 Hansen, J. S. et al. Perilipin 1 binds to aquaporin 7 in human adipocytes and controls its mobility via protein kinase A mediated phosphorylation. Metabolism 65, 1731-1742, doi:https://doi.org/10.1016/j.metabol.2016.09.004 (2016).

5 Shen, W. J., Patel, S., Miyoshi, H., Greenberg, A. S. & Kraemer, F. B. Functional interaction of hormone-sensitive lipase and perilipin in lipolysis. J Lipid Res 50, 2306-2313, doi:10.1194/jlr.M900176-JLR200 (2009).

6 Ojha, S., Budge, H. & Symonds, M. E. in Pathobiology of Human Disease (eds Linda M. McManus & Richard N. Mitchell) 2003-2013 (Academic Press, 2014).

7 Yang, A. & Mottillo, E. P. Adipocyte lipolysis: from molecular mechanisms of regulation to disease and therapeutics. Biochemical Journal 477, 985-1008, doi:10.1042/bcj20190468 (2020).

8 Suchacki, K. J. & Stimson, R. H. Nutritional Regulation of Human Brown Adipose Tissue. Nutrients 13, 1748 (2021).

9 Kwok, K. H. M., Lam, K. S. L. & Xu, A. Heterogeneity of white adipose tissue: molecular basis and clinical implications. Exp Mol Med 48, e215-e215, doi:10.1038/emm.2016.5 (2016).

10 Chait, A. & den Hartigh, L. J. Adipose Tissue Distribution, Inflammation and Its Metabolic Consequences, Including Diabetes and Cardiovascular Disease. Frontiers in Cardiovascular Medicine 7, doi:10.3389/fcvm.2020.00022 (2020).

11 Hansen, J. S., de Maré, S., Jones, H. A., Göransson, O. & Lindkvist-Petersson, K. Visualization of lipid directed dynamics of perilipin 1 in human primary adipocytes. Scientific Reports 7, 15011, doi:10.1038/s41598-017-15059-4 (2017).

12 Morigny, P., Boucher, J., Arner, P. & Langin, D. Lipid and glucose metabolism in white adipocytes: pathways, dysfunction and therapeutics. Nature Reviews Endocrinology 17, 276-295, doi:10.1038/s41574-021-00471-8 (2021).

13 Possik, E., Madiraju, S. R. M. & Prentki, M. Glycerol-3-phosphate phosphatase/PGP: Role in intermediary metabolism and target for cardiometabolic diseases. Biochimie 143, 18-28, doi:https://doi.org/10.1016/j.biochi.2017.08.001 (2017).

14 Cole, A. S. & Eastoe, J. E. in Biochemistry and Oral Biology (Second Edition) (eds A. S. Cole & J. E. Eastoe) 90-99 (Butterworth-Heinemann, 1988).

15 Guo, X. et al. Glycolysis in the control of blood glucose homeostasis. Acta Pharmaceutica Sinica B 2, 358-367, doi:https://doi.org/10.1016/j.apsb.2012.06.002 (2012).

16 Fu, X. et al. Mechanistic Study of Human Glucose Transport Mediated by GLUT1. J Chem Inf Model 56, 517-526, doi:10.1021/acs.jcim.5b00597 (2016).

17 Mueckler, M. & Thorens, B. The SLC2 (GLUT) family of membrane transporters. Mol Aspects Med 34, 121-138, doi:10.1016/j.mam.2012.07.001 (2013).

18 Leto, D. & Saltiel, A. R. Regulation of glucose transport by insulin: traffic control of GLUT4. Nature Reviews Molecular Cell Biology 13, 383-396, doi:10.1038/nrm3351 (2012).

19 Montel-Hagen, A. et al. The Glut1 and Glut4 glucose transporters are differentially expressed during perinatal and postnatal erythropoiesis. Blood 112, 4729-4738, doi:10.1182/blood-2008-05-159269 (2008).

20 Maher, F., Vannucci, S. J. & Simpson, I. A. Glucose transporter proteins in brain. Faseb j 8, 1003-1011, doi:10.1096/fasebj.8.13.7926364 (1994).

21 Beg, M., Abdullah, N., Thowfeik, F. S., Altorki, N. K. & McGraw, T. E. Distinct Akt phosphorylation states are required for insulin regulated Glut4 and Glut1-mediated glucose uptake. Elife 6, doi:10.7554/eLife.26896 (2017).

22 Szablewski, L. Expression of glucose transporters in cancers. Biochim Biophys Acta 1835, 164-169, doi:10.1016/j.bbcan.2012.12.004 (2013).

23 Grover-McKay, M., Walsh, S. A. & Thompson, S. A. Glucose transporter 3 (GLUT3) protein is present in human myocardium. Bba-Biomembranes 1416, 145-154, doi:Doi 10.1016/S0005-2736(98)00216-8 (1999).

24 Maher, F. & Simpson, I. A. Modulation of Expression of Glucose Transporters Glut3 and Glut1 by Potassium and N-Methyl-D-Aspartate in Cultured Cerebellar Granule Neurons. Mol Cell Neurosci 5, 369-375, doi:DOI 10.1006/mcne.1994.1044 (1994).

25 Thorens, B. & Mueckler, M. Glucose transporters in the 21st Century. Am J Physiol Endocrinol Metab 298, E141-E145, doi:10.1152/ajpendo.00712.2009 (2010).

26 Simmons, R. A. in Fetal and Neonatal Physiology (Fourth Edition) (eds Richard A. Polin, William W. Fox, & Steven H. Abman) 560-568 (W.B. Saunders, 2011).

27 Warburg, O. On the origin of cancer cells. Science 123, 309-314, doi:10.1126/science.123.3191.309 (1956).

28 Brewer, P. D., Habtemichael, E. N., Romenskaia, I., Mastick, C. C. & Coster, A. C. Insulin-regulated Glut4 translocation: membrane protein trafficking with six distinctive steps. J Biol Chem 289, 17280-17298, doi:10.1074/jbc.M114.555714 (2014).

29 Hanson, R. W. & Reshef, L. Glyceroneogenesis revisited. Biochimie 85, 1199-1205, doi:https://doi.org/10.1016/j.biochi.2003.10.022 (2003).

30 Song, Z., Xiaoli, A. M. & Yang, F. Regulation and Metabolic Significance of De Novo Lipogenesis in Adipose Tissues. Nutrients 10, doi:10.3390/nu10101383 (2018).

31 Zechner, R. et al. FAT SIGNALS--lipases and lipolysis in lipid metabolism and signaling. Cell Metab 15, 279-291, doi:10.1016/j.cmet.2011.12.018 (2012).

32 Prentki, M. & Madiraju, S. R. Glycerolipid/free fatty acid cycle and islet beta-cell function in health, obesity and diabetes. Mol Cell Endocrinol 353, 88-100, doi:10.1016/j.mce.2011.11.004 (2012).

33 Possik, E. et al. New Mammalian Glycerol-3-Phosphate Phosphatase: Role in beta-Cell, Liver and Adipocyte Metabolism. Front Endocrinol (Lausanne) 12, 706607, doi:10.3389/fendo.2021.706607 (2021).

34 Yeste, M., Morató, R., Rodríguez-Gil, J. E., Bonet, S. & Prieto-Martínez, N. Aquaporins in the male reproductive tract and sperm: Functional implications and cryobiology. Reprod Domest Anim 52 Suppl 4, 12-27, doi:10.1111/rda.13082 (2017).

35 Kishida, K. et al. Aquaporin adipose, a putative glycerol channel in adipocytes. J Biol Chem 275, 20896-20902, doi:10.1074/jbc.M001119200 (2000).

36 de Maré, S. W., Venskutonytė, R., Eltschkner, S., de Groot, B. L. & Lindkvist-Petersson, K. Structural Basis for Glycerol Efflux and Selectivity of Human Aquaporin 7. Structure 28, 215-222.e213, doi:https://doi.org/10.1016/j.str.2019.11.011 (2020).

37 Rodríguez, A., Catalán, V., Gómez-Ambrosi, J. & Frühbeck, G. Aquaglyceroporins serve as metabolic gateways in adiposity and insulin resistance control. Cell Cycle 10, 1548-1556, doi:10.4161/cc.10.10.15672 (2011).

38 Laforenza, U., Scaffino, M. F. & Gastaldi, G. Aquaporin-10 represents an alternative pathway for glycerol efflux from human adipocytes. PLoS One 8, e54474, doi:10.1371/journal.pone.0054474 (2013).

39 Agre, P. et al. Aquaporin CHIP: the archetypal molecular water channel. American Journal of Physiology-Renal Physiology 265, F463-F476, doi:10.1152/ajprenal.1993.265.4.F463 (1993).

40 Maunsbach, A. B. et al. Aquaporin-1 water channel expression in human kidney. J Am Soc Nephrol 8, 1-14, doi:10.1681/asn.V811 (1997).

41 Gual, P. et al. Hyperosmotic stress inhibits insulin receptor substrate-1 function by distinct mechanisms in 3T3-L1 adipocytes. J Biol Chem 278, 26550-26557, doi:10.1074/jbc.M212273200 (2003).

42 Madonna, R., Montebello, E., Lazzerini, G., Zurro, M. & De Caterina, R. NA+/H+ exchanger 1- and aquaporin-1-dependent hyperosmolarity changes decrease nitric oxide production and induce VCAM-1 expression in endothelial cells exposed to high glucose. Int J Immunopathol Pharmacol 23, 755-765, doi:10.1177/039463201002300309 (2010).

43 Madonna, R. et al. Simulated hyperglycemia impairs insulin signaling in endothelial cells through a hyperosmolar mechanism. Vascul Pharmacol 130, 106678, doi:10.1016/j.vph.2020.106678 (2020).

44 Zhang, H. & Verkman, A. S. Aquaporin-1 tunes pain perception by interaction with Na(v)1.8 Na+ channels in dorsal root ganglion neurons. J Biol Chem 285, 5896-5906, doi:10.1074/jbc.M109.090233 (2010).

45 Zhang, W. et al. Aquaporin-1 channel function is positively regulated by protein kinase C. J Biol Chem 282, 20933-20940, doi:10.1074/jbc.M703858200 (2007).

46 Lebeck, J. Metabolic impact of the glycerol channels AQP7 and AQP9 in adipose tissue and liver. Journal of Molecular Endocrinology 52, R165-R178, doi:10.1530/jme-13-0268 (2014).

47 Sugiyama, Y., Ota, Y., Hara, M. & Inoue, S. Osmotic stress up-regulates aquaporin-3 gene expression in cultured human keratinocytes. Biochim Biophys Acta 1522, 82-88, doi:10.1016/s0167-4781(01)00320-7 (2001).

48 Matsuzaki, T., Suzuki, T., Koyama, H., Tanaka, S. & Takata, K. Water channel protein AQP3 is present in epithelia exposed to the environment of possible water loss. J Histochem Cytochem 47, 1275-1286, doi:10.1177/002215549904701007 (1999).

49 Mobasheri, A., Wray, S. & Marples, D. Distribution of AQP2 and AQP3 water channels in human tissue microarrays. J Mol Histol 36, 1-14, doi:10.1007/s10735-004-2633-4 (2005).

50 Silberstein, C. et al. Functional characterization and localization of AQP3 in the human colon. Braz J Med Biol Res 32, 1303-1313, doi:10.1590/s0100-879x1999001000018 (1999).

51 Rodríguez, A. et al. Insulin- and Leptin-Mediated Control of Aquaglyceroporins in Human Adipocytes and Hepatocytes Is Mediated via the PI3K/Akt/mTOR Signaling Cascade. The Journal of Clinical Endocrinology & Metabolism 96, E586-E597, doi:10.1210/jc.2010-1408 (2011).

52 Carbrey, J. M. et al. Aquaglyceroporin AQP9: solute permeation and metabolic control of expression in liver. Proc Natl Acad Sci U S A 100, 2945-2950, doi:10.1073/pnas.0437994100 (2003).

53 Elkjaer, M. et al. Immunolocalization of AQP9 in liver, epididymis, testis, spleen, and brain. Biochem Biophys Res Commun 276, 1118-1128, doi:10.1006/bbrc.2000.3505 (2000).

54 Ishibashi, K. et al. Cloning and functional expression of a new aquaporin (AQP9) abundantly expressed in the peripheral leukocytes permeable to water and urea, but not to glycerol. Biochem Biophys Res Commun 244, 268-274, doi:10.1006/bbrc.1998.8252 (1998).

55 Karlsson, T. et al. Aquaporin 9 phosphorylation mediates membrane localization and neutrophil polarization. J Leukoc Biol 90, 963-973, doi:10.1189/jlb.0910540 (2011).

56 Ishibashi, K., Morinaga, T., Kuwahara, M., Sasaki, S. & Imai, M. Cloning and identification of a new member of water channel (AQP10) as an aquaglyceroporin. Biochim Biophys Acta 1576, 335-340, doi:10.1016/s0167-4781(02)00393-7 (2002).

57 Gotfryd, K. et al. Human adipose glycerol flux is regulated by a pH gate in AQP10. Nature Communications 9, 4749, doi:10.1038/s41467-018-07176-z (2018).

58 Braun, P. & Gingras, A. C. History of protein-protein interactions: from egg-white to complex networks. Proteomics 12, 1478-1498, doi:10.1002/pmic.201100563 (2012).

59 Bogan, J. S., Hendon, N., McKee, A. E., Tsao, T. S. & Lodish, H. F. Functional cloning of TUG as a regulator of GLUT4 glucose transporter trafficking. Nature 425, 727-733, doi:10.1038/nature01989 (2003).

60 Waldhart, A. N. et al. Phosphorylation of TXNIP by AKT Mediates Acute Influx of Glucose in Response to Insulin. Cell Rep 19, 2005-2013, doi:10.1016/j.celrep.2017.05.041 (2017).

61 Dotimas, J. R. et al. Diabetes regulates fructose absorption through thioredoxin-interacting protein. Elife 5, doi:10.7554/eLife.18313 (2016).

62 Reichow, S. L. & Gonen, T. Noncanonical binding of calmodulin to aquaporin-0: implications for channel regulation. Structure 16, 1389-1398, doi:10.1016/j.str.2008.06.011 (2008).

63 van Balkom, B. W. M. et al. LIP5 interacts with aquaporin 2 and facilitates its lysosomal degradation. Journal of the American Society of Nephrology : JASN 20, 990-1001, doi:10.1681/ASN.2008060648 (2009).

64 Chivasso, C. et al. Unraveling Human AQP5-PIP Molecular Interaction and Effect on AQP5 Salivary Glands Localization in SS Patients. Cells 10, doi:10.3390/cells10082108 (2021).

65 Buchberger, A., Howard, M. J., Proctor, M. & Bycroft, M. The UBX domain: a widespread ubiquitin-like module. J Mol Biol 307, 17-24, doi:10.1006/jmbi.2000.4462 (2001).

66 Shido, Y. & Matsuyama, Y. Advanced Alveolar Soft Part Sarcoma Treated with Pazopanib over Three Years. Case Reports in Oncological Medicine 2017 (2017).

67 Arumughan, A. et al. Quantitative interaction mapping reveals an extended UBX domain in ASPL that disrupts functional p97 hexamers. Nature Communications 7, 13047, doi:10.1038/ncomms13047 (2016).

68 Jumper, J. et al. Highly accurate protein structure prediction with AlphaFold. Nature 596, 583-589, doi:10.1038/s41586-021-03819-2 (2021).

69 Tettamanzi, M. C., Yu, C., Bogan, J. S. & Hodsdon, M. E. Solution structure and backbone dynamics of an N-terminal ubiquitin-like domain in the GLUT4-regulating protein, TUG. Protein Sci 15, 498-508, doi:10.1110/ps.051901806 (2006).

70 Bogan, J. S. et al. Endoproteolytic cleavage of TUG protein regulates GLUT4 glucose transporter translocation. J Biol Chem 287, 23932-23947, doi:10.1074/jbc.M112.339457 (2012).

71 Londos, C., Brasaemle, D. L., Schultz, C. J., Segrest, J. P. & Kimmel, A. R. Perilipins, ADRP, and other proteins that associate with intracellular neutral lipid droplets in animal cells. Semin Cell Dev Biol 10, 51-58, doi:10.1006/scdb.1998.0275 (1999).

72 Rowe, E. R. et al. Conserved Amphipathic Helices Mediate Lipid Droplet Targeting of Perilipins 1-3. J Biol Chem 291, 6664-6678, doi:10.1074/jbc.M115.691048 (2016).

73 Gandotra, S. et al. Human frame shift mutations affecting the carboxyl terminus of perilipin increase lipolysis by failing to sequester the adipose triglyceride lipase (ATGL) coactivator AB-hydrolase-containing 5 (ABHD5). J Biol Chem 286, 34998-35006, doi:10.1074/jbc.M111.278853 (2011).

74 Sztalryd, C. & Brasaemle, D. L. The perilipin family of lipid droplet proteins: Gatekeepers of intracellular lipolysis. Biochim Biophys Acta Mol Cell Biol Lipids 1862, 1221-1232, doi:10.1016/j.bbalip.2017.07.009 (2017).

75 Nesverova, V. & Törnroth-Horsefield, S. Phosphorylation-Dependent Regulation of Mammalian Aquaporins. Cells 8, doi:10.3390/cells8020082 (2019).

76 Deng, D. et al. Crystal structure of the human glucose transporter GLUT1. Nature 510, 121-125, doi:10.1038/nature13306 (2014).

77 Deng, D. et al. Molecular basis of ligand recognition and transport by glucose transporters. Nature 526, 391-396, doi:10.1038/nature14655 (2015).

78 Nomura, N. et al. Structure and mechanism of the mammalian fructose transporter GLUT5. Nature 526, 397-401, doi:10.1038/nature14909 (2015).

79 Kotov, V. et al. High-throughput stability screening for detergent-solubilized membrane proteins. Scientific Reports 9, 10379, doi:10.1038/s41598-019-46686-8 (2019).

80 Vander Heiden, M. G., Cantley, L. C. & Thompson, C. B. Understanding the Warburg effect: the metabolic requirements of cell proliferation. Science 324, 1029-1033, doi:10.1126/science.1160809 (2009).

81 Medina, R. A. & Owen, G. I. Glucose transporters: expression, regulation and cancer. Biol Res 35, 9-26, doi:10.4067/s0716-97602002000100004 (2002).

82 Pliszka, M. & Szablewski, L. Glucose Transporters as a Target for Anticancer Therapy. Cancers 13, 4184 (2021).

83 Chan, D. A. et al. Targeting GLUT1 and the Warburg effect in renal cell carcinoma by chemical synthetic lethality. Sci Transl Med 3, 94ra70, doi:10.1126/scitranslmed.3002394 (2011).

84 Ojelabi, O. A., Lloyd, K. P., Simon, A. H., De Zutter, J. K. & Carruthers, A. WZB117 (2-Fluoro-6-(m-hydroxybenzoyloxy) Phenyl m-Hydroxybenzoate) Inhibits GLUT1-mediated Sugar Transport by Binding Reversibly at the Exofacial Sugar Binding Site. J Biol Chem 291, 26762-26772, doi:10.1074/jbc.M116.759175 (2016).

85 Siebeneicher, H. et al. Identification and Optimization of the First Highly Selective GLUT1 Inhibitor BAY-876. ChemMedChem 11, 2261-2271, doi:10.1002/cmdc.201600276 (2016).

86 Granchi, C. et al. Salicylketoximes That Target Glucose Transporter 1 Restrict Energy Supply to Lung Cancer Cells. ChemMedChem 10, 1892-1900, doi:10.1002/cmdc.201500320 (2015).

87 Carruthers, A. ATP regulation of the human red cell sugar transporter. J Biol Chem 261, 11028-11037 (1986).

88 Kraft, T. E., Hresko, R. C. & Hruz, P. W. Expression, purification, and functional characterization of the insulin-responsive facilitative glucose transporter GLUT4. Protein Sci 24, 2008-2019, doi:10.1002/pro.2812 (2015).

89 Murata, K. et al. Structural determinants of water permeation through aquaporin-1. Nature 407, 599-605, doi:10.1038/35036519 (2000).

90 Frick, A. et al. X-ray structure of human aquaporin 2 and its implications for nephrogenic diabetes insipidus and trafficking. Proceedings of the National Academy of Sciences 111, 6305-6310, doi:10.1073/pnas.1321406111 (2014).

91 Ho, J. D. et al. Crystal structure of human aquaporin 4 at 1.8 Å and its mechanism of conductance. Proceedings of the National Academy of Sciences 106, 7437-7442, doi:10.1073/pnas.0902725106 (2009).

92 Horsefield, R. et al. High-resolution x-ray structure of human aquaporin 5. Proceedings of the National Academy of Sciences 105, 13327-13332, doi:10.1073/pnas.0801466105 (2008).

93 Sui, H., Han, B.-G., Lee, J. K., Walian, P. & Jap, B. K. Structural basis of water-specific transport through the AQP1 water channel. Nature 414, 872-878, doi:10.1038/414872a (2001).

94 Yu, J., Yool, A. J., Schulten, K. & Tajkhorshid, E. Mechanism of gating and ion conductivity of a possible tetrameric pore in aquaporin-1. Structure 14, 1411-1423, doi:10.1016/j.str.2006.07.006 (2006).

95 Roche, J. V. & Törnroth-Horsefield, S. Aquaporin Protein-Protein Interactions. International journal of molecular sciences 18, 2255, doi:10.3390/ijms18112255 (2017).

96 Moss, F. J. et al. Aquaporin-7: A Dynamic Aquaglyceroporin With Greater Water and Glycerol Permeability Than Its Bacterial Homolog GlpF. Front Physiol 11, 728-728, doi:10.3389/fphys.2020.00728 (2020).

97 Shoemaker, S. C. & Ando, N. X-rays in the Cryo-Electron Microscopy Era: Structural Biology's Dynamic Future. Biochemistry 57, 277-285, doi:10.1021/acs.biochem.7b01031 (2018).

98 Yool, A. J., Stamer, W. D. & Regan, J. W. Forskolin stimulation of water and cation permeability in aquaporin 1 water channels. Science 273, 1216-1218, doi:10.1126/science.273.5279.1216 (1996).

99 Anthony, T. L. et al. Cloned Human Aquaporin-1 Is a Cyclic GMP-Gated Ion Channel. Molecular Pharmacology 57, 576-588, doi:10.1124/mol.57.3.576 (2000).

100 Yool, A. J. & Weinstein, A. M. New roles for old holes: ion channel function in aquaporin-1. News Physiol Sci 17, 68-72, doi:10.1152/nips.01372.2001 (2002).

101 Boassa, D., Stamer, W. D. & Yool, A. J. Ion channel function of aquaporin-1 natively expressed in choroid plexus. J Neurosci 26, 7811-7819, doi:10.1523/jneurosci.0525-06.2006 (2006).

102 Wang, Y., Cohen, J., Boron, W. F., Schulten, K. & Tajkhorshid, E. Exploring gas permeability of cellular membranes and membrane channels with molecular dynamics. J Struct Biol 157, 534-544, doi:10.1016/j.jsb.2006.11.008 (2007).

103 Horsefield, R. et al. High-resolution x-ray structure of human aquaporin 5. Proc Natl Acad Sci U S A 105, 13327-13332, doi:10.1073/pnas.0801466105 (2008).

104 Wang, Q., Quan, S. & Xiao, H. Towards efficient terpenoid biosynthesis: manipulating IPP and DMAPP supply. Bioresources and Bioprocessing 6, 6, doi:10.1186/s40643-019-0242-z (2019).

105 Costello, M. J., McIntosh, T. J. & Robertson, J. D. Distribution of gap junctions and square array junctions in the mammalian lens. Invest Ophthalmol Vis Sci 30, 975-989 (1989).

106 Gonen, T. et al. Lipid-protein interactions in double-layered two-dimensional AQP0 crystals (vol 438, pg 633, 2005). Nature 441, 248-248, doi:10.1038/nature04775 (2006).

107 Hiroaki, Y. et al. Implications of the aquaporin-4 structure on array formation and cell adhesion. Journal of Molecular Biology 355, 628-639, doi:10.1016/j.jmb.2005.10.081 (2006).

108 Gonen, T., Cheng, Y., Kistler, J. & Walz, T. Aquaporin-0 membrane junctions form upon proteolytic cleavage. Journal of Molecular Biology 342, 1337-1345, doi:10.1016/j.jmb.2004.07.076 (2004).

109 Lemieux, M. J., Huang, Y. & Wang, D.-N. Glycerol-3-phosphate transporter of Escherichia coli: Structure, function and regulation. Research in Microbiology 155, 623-629, doi:https://doi.org/10.1016/j.resmic.2004.05.016 (2004).

110 Aikman, B., de Almeida, A., Meier-Menches, S. M. & Casini, A. Aquaporins in cancer development: opportunities for bioinorganic chemistry to contribute novel chemical probes and therapeutic agents. Metallomics 10, 696-712, doi:10.1039/c8mt00072g (2018).

111 Hara-Chikuma, M. & Verkman, A. S. Prevention of skin tumorigenesis and impairment of epidermal cell proliferation by targeted aquaporin-3 gene disruption. Mol Cell Biol 28, 326-332, doi:10.1128/mcb.01482-07 (2008).

112 Xia, H. et al. Aquaporin 3 knockdown suppresses tumour growth and angiogenesis in experimental non-small cell lung cancer. Exp Physiol 99, 974-984, doi:10.1113/expphysiol.2014.078527 (2014).

113 Satooka, H. & Hara-Chikuma, M. Aquaporin-3 Controls Breast Cancer Cell Migration by Regulating Hydrogen Peroxide Transport and Its Downstream Cell Signaling. Mol Cell Biol 36, 1206-1218, doi:10.1128/mcb.00971-15 (2016).

114 Dai, C. et al. Aquaporin-7 Regulates the Response to Cellular Stress in Breast Cancer. Cancer Res 80, 4071-4086, doi:10.1158/0008-5472.CAN-19-2269 (2020).

115 MacDougald, O. A. & Burant, C. F. Obesity and metabolic perturbations after loss of aquaporin 7, the adipose glycerol transporter. Proceedings of the National Academy of Sciences of the United States of America 102, 10759-10760, doi:10.1073/pnas.0504965102 (2005).

116 Baeshen, M. N. et al. Production of Biopharmaceuticals in E. coli: Current Scenario and Future Perspectives. J Microbiol Biotechnol 25, 953-962, doi:10.4014/jmb.1412.12079 (2015).

117 Gupta, S. K., Dangi, A. K., Smita, M., Dwivedi, S. & Shukla, P. in Applied Microbiology and Bioengineering (ed Pratyoosh Shukla) 203-227 (Academic Press, 2019).

118 Routledge, S. J. et al. The synthesis of recombinant membrane proteins in yeast for structural studies. Methods 95, 26-37, doi:https://doi.org/10.1016/j.ymeth.2015.09.027 (2016).

119 Macauley-Patrick, S., Fazenda, M. L., McNeil, B. & Harvey, L. M. Heterologous protein production using the Pichia pastoris expression system. Yeast 22, 249-270, doi:10.1002/yea.1208 (2005).

120 Arya, R., Bhattacharya, A. & Saini, K. S. Dictyostelium discoideum—a promising expression system for the production of eukaryotic proteins. The FASEB Journal 22, 4055-4066, doi:https://doi.org/10.1096/fj.08-110544 (2008).

121 Wildt, S. & Gerngross, T. U. The humanization of N-glycosylation pathways in yeast. Nat Rev Microbiol 3, 119-128, doi:10.1038/nrmicro1087 (2005).

122 Boswell-Casteel, R. C., Johnson, J. M., Stroud, R. M. & Hays, F. A. Integral Membrane Protein Expression in Saccharomyces cerevisiae. Methods Mol Biol 1432, 163-186, doi:10.1007/978-1-4939-3637-3_11 (2016).

123 Custódio, T. F., Paulsen, P. A., Frain, K. M. & Pedersen, B. P. Structural comparison of GLUT1 to GLUT3 reveal transport regulation mechanism in sugar porter family. Life Science Alliance 4, e202000858, doi:10.26508/lsa.202000858 (2021).

124 Ikonomou, L., Schneider, Y. J. & Agathos, S. N. Insect cell culture for industrial production of recombinant proteins. Appl Microbiol Biotechnol 62, 1-20, doi:10.1007/s00253-003-1223-9 (2003).

125 He, Y., Wang, K. & Yan, N. The recombinant expression systems for structure determination of eukaryotic membrane proteins. Protein Cell 5, 658-672, doi:10.1007/s13238-014-0086-4 (2014).

126 Walsh, B. W., Lenhart, J. S., Schroeder, J. W. & Simmons, L. A. Far Western blotting as a rapid and efficient method for detecting interactions between DNA replication and DNA repair proteins. Methods Mol Biol 922, 161-168, doi:10.1007/978-1-62703-032-8_11 (2012).

127 Killinger, B. A. & Moszczynska, A. Characterization of α-Synuclein Multimer Stoichiometry in Complex Biological Samples by Electrophoresis. Analytical Chemistry 88, 4071-4084, doi:10.1021/acs.analchem.6b00419 (2016).

128 Podobnik, M. et al. How to Study Protein-protein Interactions. Acta Chim Slov 63, 424-439, doi:10.17344/acsi.2016.2419 (2016).

129 Mintseris, J. & Gygi, S. P. High-density chemical cross-linking for modeling protein interactions. Proceedings of the National Academy of Sciences 117, 93-102, doi:10.1073/pnas.1902931116 (2020).

130 Amiry-Moghaddam, M. & Ottersen, O. P. Immunogold cytochemistry in neuroscience. Nature Neuroscience 16, 798-804, doi:10.1038/nn.3418 (2013).

131 Sternberger, L. A., Donati, E. J., Cuculis, J. J. & Petrali, J. P. INDIRECT IMMUNOURANIUM TECHNIQUE FOR STAINING OF EMBEDDED ANTIGEN IN ELECTRON MICROSCOPY. Exp Mol Pathol 4, 112-125, doi:10.1016/0014-4800(65)90027-4 (1965).

132 Singer, S. J. Preparation of an electron-dense antibody conjugate. Nature 183, 1523-1524, doi:10.1038/1831523a0 (1959).

133 Dutton, A. H., Tokuyasu, K. T. & Singer, S. J. Iron-dextran antibody conjugates: General method for simultaneous staining of two components in high-resolution immunoelectron microscopy. Proc Natl Acad Sci U S A 76, 3392-3396, doi:10.1073/pnas.76.7.3392 (1979).

134 Hermann, R., Walther, P. & Müller, M. Immunogold labeling in scanning electron microscopy. Histochemistry and Cell Biology 106, 31-39, doi:10.1007/BF02473200 (1996).

135 Baschong, W. & Aebi, U. in Cell Biology (Third Edition) (ed Julio E. Celis) 233-240 (Academic Press, 2006).

136 Scarff, C. A., Fuller, M. J. G., Thompson, R. F. & Iadanza, M. G. Variations on Negative Stain Electron Microscopy Methods: Tools for Tackling Challenging Systems. J Vis Exp, 57199, doi:10.3791/57199 (2018).

137 Ohi, M., Li, Y., Cheng, Y. & Walz, T. Negative Staining and Image Classification - Powerful Tools in Modern Electron Microscopy. Biol Proced Online 6, 23-34, doi:10.1251/bpo70 (2004).

138 Hebert, H. CryoEM: a crystals to single particles round-trip. Curr Opin Struct Biol 58, 59-67, doi:https://doi.org/10.1016/j.sbi.2019.05.008 (2019).

139 Dobro, M. J., Melanson, L. A., Jensen, G. J. & McDowall, A. W. in Methods in Enzymology Vol. 481 (ed Grant J. Jensen) 63-82 (Academic Press, 2010).

140 Punjani, A., Rubinstein, J. L., Fleet, D. J. & Brubaker, M. A. cryoSPARC: algorithms for rapid unsupervised cryo-EM structure determination. Nature Methods 14, 290-296, doi:10.1038/nmeth.4169 (2017).

141 Zivanov, J. et al. New tools for automated high-resolution cryo-EM structure determination in RELION-3. eLife 7, e42166, doi:10.7554/eLife.42166 (2018).

142 Brito, J. A. & Archer, M. in Practical Approaches to Biological Inorganic Chemistry (Second Edition) (eds Robert R. Crichton & Ricardo O. Louro) 375-416 (Elsevier, 2020).

143 Wang, H. W. & Wang, J. W. How cryo-electron microscopy and X-ray crystallography complement each other. Protein Sci 26, 32-39, doi:10.1002/pro.3022 (2017).

144 Liu, Y., Huynh, D. T. & Yeates, T. O. A 3.8 Å resolution cryo-EM structure of a small protein bound to an imaging scaffold. Nature Communications 10, 1864, doi:10.1038/s41467-019-09836-0 (2019).

145 Autzen, H. E., Julius, D. & Cheng, Y. Membrane mimetic systems in CryoEM: keeping membrane proteins in their native environment. Curr Opin Struct Biol 58, 259-268, doi:10.1016/j.sbi.2019.05.022 (2019).

146 Breyton, C., Chabaud, E., Chaudier, Y., Pucci, B. & Popot, J.-L. Hemifluorinated surfactants: a non-dissociating environment for handling membrane proteins in aqueous solutions? FEBS Letters 564, 312-318, doi:https://doi.org/10.1016/S0014-5793(04)00227-3 (2004).

147 Tribet, C., Audebert, R. & Popot, J. L. Amphipols: polymers that keep membrane proteins soluble in aqueous solutions. Proc Natl Acad Sci U S A 93, 15047-15050, doi:10.1073/pnas.93.26.15047 (1996).

148 Popot, J. L. et al. Amphipols from A to Z. Annu Rev Biophys 40, 379-408, doi:10.1146/annurev-biophys-042910-155219 (2011).

149 Calabrese, A. N., Watkinson, T. G., Henderson, P. J. F., Radford, S. E. & Ashcroft, A. E. Amphipols Outperform Dodecylmaltoside Micelles in Stabilizing Membrane Protein Structure in the Gas Phase. Analytical Chemistry 87, 1118-1126, doi:10.1021/ac5037022 (2015).

150 Le Bon, C., Marconnet, A., Masscheleyn, S., Popot, J.-L. & Zoonens, M. Folding and stabilizing membrane proteins in amphipol A8-35. Methods 147, 95-105, doi:https://doi.org/10.1016/j.ymeth.2018.04.012 (2018).

151 Pocanschi, C. L. et al. Amphipathic polymers: tools to fold integral membrane proteins to their active form. Biochemistry 45, 13954-13961, doi:10.1021/bi0616706 (2006).

Acknowledgement

It is 22:53 at 25th of November, Thanksgiving Day. The night is quiet, and all scenarios occurred from the day when I came to Lund flash quickly through my mind like silent films. Then I realize it is time to finish this section formally and grandly “giving my sincere thanks to all of you”.

First and foremost, I give my most thanks to my supervisor, **Karin**, who always provides me patient teaching and good suggestions on my projects, even when I did not know anything when I started my PhD. Your positive and optimistic attitude towards life and work really eases my stress especially when I came to a strange country at first time in my life, faced with two super challengeable projects and did not show any competence for structure biological projects at first, and makes me believe “never give up”. Also, thanks for your training for my skills on the aspects of language, scientific communication, and writing. Scientific research is never one dimension. Then I would thank my smart and kind co-supervisor, **Pontus**. You can always find the point and give me useful comments for problems I encountered in the project, particularly when the structure came. It is really a happy thing that my co-supervisor was sitting the same office with me.

I am so lucky that I met these super nice colleagues in the lab, who brought me happiness, warmth, encouragement, and help. Many thanks for **Ping**. I am very grateful for your continuous support and help on my life and work from the first day when I arrived BMC, specifically for your experience and suggestions on protein purification and structural analysis. I am really appreciated to have a “Senior” in the lab who was doing the relevant projects as me, and hard to know how much time has been saved by adopting your suggestions. Thank you, my senior, **Raminta**, and say hello to my little junior. **Sibel**, I do not really remember how much days we did not greet each other as routine by “exciting/amazing/funny day?”. I understand how stressful we are experiencing in this last year, but not forget those happy time in previous years we spent together. I always think what a pleasure to be your colleague and friend, **Niloofar**, you are such a nice and warm person, thanks a lot for your help and encouragement through four years, and your yummy chocolates. I am really appreciated that you always have sweet smile on the face whenever I meet you, **Hannah**, and I feel all the time very relaxed and natural when talking with you, just like many-year friends. Thanks! **Philippa**, welcome you join in the group and sharing the office with us. In addition, I would like to acknowledge those colleagues who have left from the lab, **Sofia** (Sam’s grandma, so pity missing your

defence), **Serena** (my first teacher on protein purification and crystallization), **Jesper** (biochemical assays are that difficult when you left) as well as **Kamil**, **Christian**, **Julia**, **Charlie**. Also, my neighboring colleagues left already, **Jens**, **Rita**, **Okta**, thanks for your help and talks especially when I was fresh here. **Pal** and **Markel**, many thanks for your help and suggestions on cryo-EM data analysis and process. Additionally, thanks **Ton**, my nice neighbor, I am enjoyed for all greeting and talks with you, and **Minjun**, thanks for your patient instructions on computer issues, and **Qirui**, hope you have a happy life in new country, as well as **Karim**, **Maria**, **Anna**, **Helena**, **Somadri**, and all other colleagues in clinical genetic. Welcome and thank our new neighbors, **Vasili** who is an interesting and powerful researcher and his group members. Also appreciated for the talk, and help, or collaboration involved in the project from those colleagues in other corridors of BMC, **Karin Stenkula**, **Jitka Petrlova**, **Lotta Hopponen**, **Charlotte Welinder**, **Hong Yan**, **Tommaso**, **Lina Gefors**, **Yang Liu**, **Xiaoxu**, **Ouyang**, **Chengjun** as well as **Ingemar**, **Susanna**, **Tamim**, **Carl**, **Derek** in KC. Thanks **Liying**, **Kaituo**, **Julie**, **Pin** and **Xiaoxia** in Copenhagen for your discussions and suggestions on the projects, and the help of **Mahmood** and **Mina** when I was visiting in Oslo. With special gratitude to **Nieng Yang** and **Xiao Fan** in Princeton University in US for your suggestions and collaboration on cryo-EM project.

Give many thanks to my Chinese friends in Lund, **LuMeng** and **GuoYing**, **HuNan**, **Guanqun**, **ZhaoLiang** and **Jiaming** and those who had left from Lund, **Dingyuan**, **Qimin**, **Meiting** and **Suxun**, and friends studying in other countries of Europe, **Zhiwei**, **LiuGang** and **ZhaoXin**, and those in China, **129** 兄弟们, 刘老师, 术亮, 兵令, 业峰, 王威…

In addition, I would like to express my acknowledgement to China Scholarship Council (**CSC**) sponsoring me to finish my PhD study. Also, thanks for study mode and work environment in **Sweden**, culturing my independent personality and thinking towards work and life, which would be a priceless treasure for my whole life.

Finally, and the most importantly, I give my special and sincere appreciation to my wife, **Chengyu**, my one and only who has changed and is changing my life, with your life wisdom, unconditional support, and selfless dedication. From the moment of boarding the flight to Sweden, I realized it would be a way full of thorns and bitterness, however, the reality is far away from what I could imagine, but with your company, I am tasting the sweet in the life. You are lighting up the dark! I am so grateful to be your husband, and I want to do everything I can to continue to make you smile and to be the man you want me to be. We are lucky, as we have a suchchchch sweet boy, **Mingche**, my "project" I feel the proudest in my PhD. Thanks for your coming. Forgive your papa that he is learning and growing with you together, but he is trying to be your superman.

此外，由衷地感谢我的父母，这是一种感谢不足以表达的感谢，一种身为人父才能理解的感谢，你们辛苦了！还有我的岳父岳母，感谢你们把你们把你们最引以为豪的女儿交给我，感谢你们对我的肯定，特别是我岳母，在我们最困难的时候，不远万里来到这里, 给予我们无私的帮助。最后还有我其他的亲人们，因为有你们在我父母身边我才会在异国他乡如此安心，衷心地感谢你们！

2021. 12. 01

Lund, Sweden